Morphology, Composition, and Ontogenesis of Platinum-Group Minerals in Chromitites of Zoned Clinopyroxenite–Dunite Massifs of the Middle Urals

S.Yu. Stepanov[a,b, ✉], R.S. Palamarchuk[b,c], A.V. Antonov[c], A.V. Kozlov[b], D.A. Varlamov[d], D.A. Khanin[d,e], A.A. Zolotarev, Jr.[f]

[a] *Zavaritsky Institute of Geology and Geochemistry, Ural Branch of the Russian Academy of Sciences, ul. Akademika Vonsovskogo 14, Yekaterinburg, 620016, Russia*

[b] *St. Petersburg Mining University, Vasil'evskii ostrov, 2-ya Liniya 2, St. Petersburg, 199106, Russia*

[c] *A.P. Karpinsky Russian Geological Research Institute, Srednii pr. 74, St. Petersburg, 199106, Russia*

[d] *Institute of Experimental Mineralogy, Russian Academy of Sciences, ul. Akad. Osip'yana 4, Chernogolovka, 142432, Russia*

[e] *Lomonosov Moscow State University, Leninskie Gory 1, Moscow, 119991, Russia*

[f] *St. Petersburg State University, Universitetskaya nab. 7/9, St. Petersburg, 199034, Russia*

Abstract—We present results of analysis of the morphology and chemical composition of platinum-group minerals from chromite–platinum orebodies of zoned clinopyroxenite–dunite massifs in the Middle Urals (Nizhnii Tagil, Svetlyi Bor, Veresovyi Bor, and Kamenushenskii). Study of more than 500 grains has given an insight into the sequence of formation of platinum-group minerals in chromitites of the studied massifs. Three assemblages of platinum-group minerals have been revealed: magmatic (Os–Ir–Ru intermetallic compounds, isoferroplatinum, ferroplatinum, sulfides of the isomorphous series erlichmanite–laurite and kashinite–bowieite, and thiospinels of the series cuproiridsite–cuprorhodsite–malanite); postmagmatic (with a predominance of tulameenite, tetraferroplatinum, and ferronickelplatinum, resulted from serpentinization of dunites); and latest secondary (minerals with a predominance of PGE sulfides, arsenides, sulfoantimonides, sulfoarsenides, plumbides, and amalgams).

INTRODUCTION

Zoned clinopyroxenite–dunite massifs, also called massifs of the Ural–Alaskan type, enclose giant (in terms of reserves) platinum placers. At the beginning of the commercial exploitation of these placers, platinum-group mineralization was not seriously investigated. Active research began only in the late 19th century, after the discovery of the first primary deposits of platinum in 1891 (Lokerman, 1982; Mosin, 2002), and its results were headlined (Karpinsky, 1893; Zaitsev, 1898; Duparc and Tikhonowich, 1920).

More than 500 tons of platinum-group metals were mined from platinum placers in the Ural region throughout their mining history (Mosin, 2002), which significantly exceeds the production of platinum from similar placers in Russia and in the world. Placers in zoned clinopyroxenite–dunite massifs are known in the Koryak–Kamchatka region (Tolstykh et al., 2005; Sidorov et al., 2012, 2019; Kutyrev et al.,

2018) Santiago River, Ecuador (Weiser and Schmidt-Thome, 1993), Durance River, France (Johan et al., 1990), Tulameen River, British Columbia (Nixon et al., 1990), and Manampotsy area, Madagascar (Legendre and Auge, 1992). There are no analogues of the Ural primary deposits with chromite–platinum mineralization in the world. In Russia, primary platinum-group mineralization was found and comprehensively studied only in dunites of the Gal'moenan massif in Koryakia (Sidorov et al., 2012).

Primary chromite–platinum mineralization in zoned clinopyroxenite–dunite massifs is an object of not only research but also geological prospecting and mining (Kashin et al., 1956). The geologic structure of these massifs, the forms of chromitite occurrence within them, the mineral composition of these rocks, and the distribution and composition of platinum-group minerals are described elsewhere (Vysotskii, 1913; Karpinsky, 1926; Zavaritskii, 1928; Betekhtin, 1935; Lazarenkov et al., 1992; Ivanov, 1997; Auge et al., 2005; Volchenko et al., 2007; Kozlov et al., 2011; Anikina et al., 2014; Malitch et al., 2015). Analysis of available research works concerned with platinum-group miner-

✉Corresponding author.
E-mail adress: Stepanov-1@yandex.ru (S.Yu. Stepanov)

alization of clinopyroxenite–dunite massifs in the Middle Urals shows that the Nizhnii Tagil massif has been most comprehensively studied. The recent geological exploration initiated by Yu.M. Telegin (Telegin et al., 2009; Tolstykh et al., 2011) has provided detailed information about the platinum-group mineral assemblages of the Svetlyi Bor and Kamenushenskii massifs.

The attention to the genesis of platinum-group mineralization was focused already at the early stages of study of the platinum content in clinopyroxenite–dunite massifs of the Urals. Early studies (Vysotskii, 1913; Duparc and Tikhonowitch, 1920; Karpinsky, 1926; Zavaritskii, 1928; Betekhtin, 1935; Kashin et al., 1956), performed along with the development of primary deposits (Gospodskaya Shakhta, Krutoi Log 4-00, and Syrkov Log), were based on representative rock material but did not lead to a consensus on the above problem. Later research (Malakhov and Malakhova, 1970; Lazarenkov et al., 1992; Ivanov, 1997; Zoloev et al., 2001; Auge et al., 2005; Pushkarev et al., 2007; Volchenko et al., 2007; Anikina et al., 2014; Tessalina et al., 2015), after the completion of the development of these deposits, was performed on the lesser number of representative samples of platinum-bearing rocks but provided an extensive analytical database. Nevertheless, a substantiated genetic concept that would be recognized by most of the researchers of these ore-bearing objects was not elaborated.

Taking into account the earlier obtained data on platinum-group minerals from zoned clinopyroxenite–dunite massifs, we analyzed and summarized data of genetic observations and a significant amount of material on the morphology of individual minerals and their aggregates. It is these ontogenetic observations that formed the basis of the genetic model of the evolution of chromite–platinum mineralization in zoned clinopyroxenite–dunite massifs of the Middle Urals.

In 2013–2017, we collected platinum-group minerals from chromitites of the least studied Svetlyi Bor, Veresovyi Bor, and Kamenushenskii clinopyroxenite–dunite massifs. This collection, along with the mineral samples from the Nizhnii Tagil massif, served as the basis for research. To confirm the results of study of bedrocks, we comprehensively examined platinum-group minerals from placers of the above massifs. The obtained data give an insight into the specific features of platinum-group mineralization in the eroded zones of the massifs and thus permit substantiation of the evolution of platinum-group mineralization using a more representative material. This material most fully characterizing the platinum-group mineralization of clinopyroxenite–dunite massifs of the Middle Urals, together with the use of the methods of genetic mineralogy and mineral ontogenesis, permits a deep analysis of the formation and subsequent transformation of platinum-group minerals in chromite–platinum ore systems.

SAMPLES AND METHODS

Cr-spinel segregations and chromitites were sampled from ore lumps in dunite bodies of the Nizhnii Tagil, Svetlyi

Bor, Veresovyi Bor, and Kamenushenskii massifs during the field works in 2013–2017 (Fig. 1). To study as more platinum-group minerals as possible, we took 27 bulk samples of chromitites (60–65 kg), crushed them to the <1 mm fraction, and enriched them using a KR-400 centrifugal concentrator. Samples of chromitites most enriched in platinum-group minerals were taken for a subsequent preparation of thin and polished sections (a total of 513). To determine the specific features of platinum-group mineralization in the eroded parts of chromite–platinum ore zones, we sampled chromitites from eluvial–deluvial and deluvial placers (more than 89 samples).

Grains and aggregates of platinum-group minerals were studied with optical binocular and scanning electron microscopes. Then, artificial polished sections of the grains were prepared, which, along with the polished thin sections of Cr-spinel segregations and chromitites, were examined with scanning electron microscopes (CamScan MX2500, Karpinsky Russian Geological Research Institute, St. Petersburg, analyst A.V. Antonov; Tescan VEGA-II XMU and CamScan MV2300, Institute of Experimental Mineralogy, Chernogolovka, analyst D.A. Varlamov; Tescan VEGA, Mining University, St. Petersburg, analyst Yu.L. Kretser). The chemical composition of platinum-group minerals was determined by X-ray probe microanalysis, using energy-dispersive microprobes (Link Pentafet, Oxford Instruments, and Si (Li), Karpinsky Russian Geological Research Institute, St. Petersburg, analyst A.V. Antonov; INCA Energy 450 and INCA Energy 350, Institute of Experimental Mineralogy, Chernogolovka, analyst D.A. Varlamov) and wave-dispersive microprobes (Camebax SX 50, Moscow State University, analyst D.A. Khanin). About 1440 analyses were carried out for ~500 grains of platinum-group minerals sampled at more than 80 points. All minerals were analyzed for six platinum-group metals, Fe, Co, Ni, and Cu, and sulfides were additionally analyzed for S, As, Sb, Te, Pb, Bi, and Hg.

The reference profiles of series of characteristic X-ray lines were recorded using the following standards for elements: PGE, pure platinum-group metals (L line); Cu, Cu_{met}; Fe, Fe_{met}; Ni, Ni_{met}; Co, CoAsS; S, FeS_{2synth}; As, InAs; Sb, $CuSbS_2$; Te, Pb, PbTe; and Bi, Bi_{met}. In X-ray probe microanalysis, the following standards were used: PGE, pure platinum group metals; Cu, Sb, $CuSbS_2$; Fe, S, FeS; Ni, NiS; Co, As, CoAsS; Hg, HgTe; Pb, PbS; and Bi, Bi_2S_3.

Measurements with a Camebax SX50 X-ray electron microprobe were made at an accelerating voltage of 20 kV and a current of 30 nA; the peaks of major elements were measured for 20 s, and the background, for 10 s from each side. The contents of impurity elements were measured for 40 s at the peaks and for 20 s at the background. The detection limits are (wt.%): Os—0.08, Ir—0.1, Ru—0.05, Rh—0.05, Pd—0.05, Pt—0.05, Fe—0.03, Ni—0.03, Cu—0.03, S—0.05, As—0.05, Co—0.03, Pb—0.08, and Bi—0.1. The contents were calculated with ZAF correction.

The phase composition of Pt–Fe minerals was confirmed by X-ray diffraction analysis on the equipment of the "X-
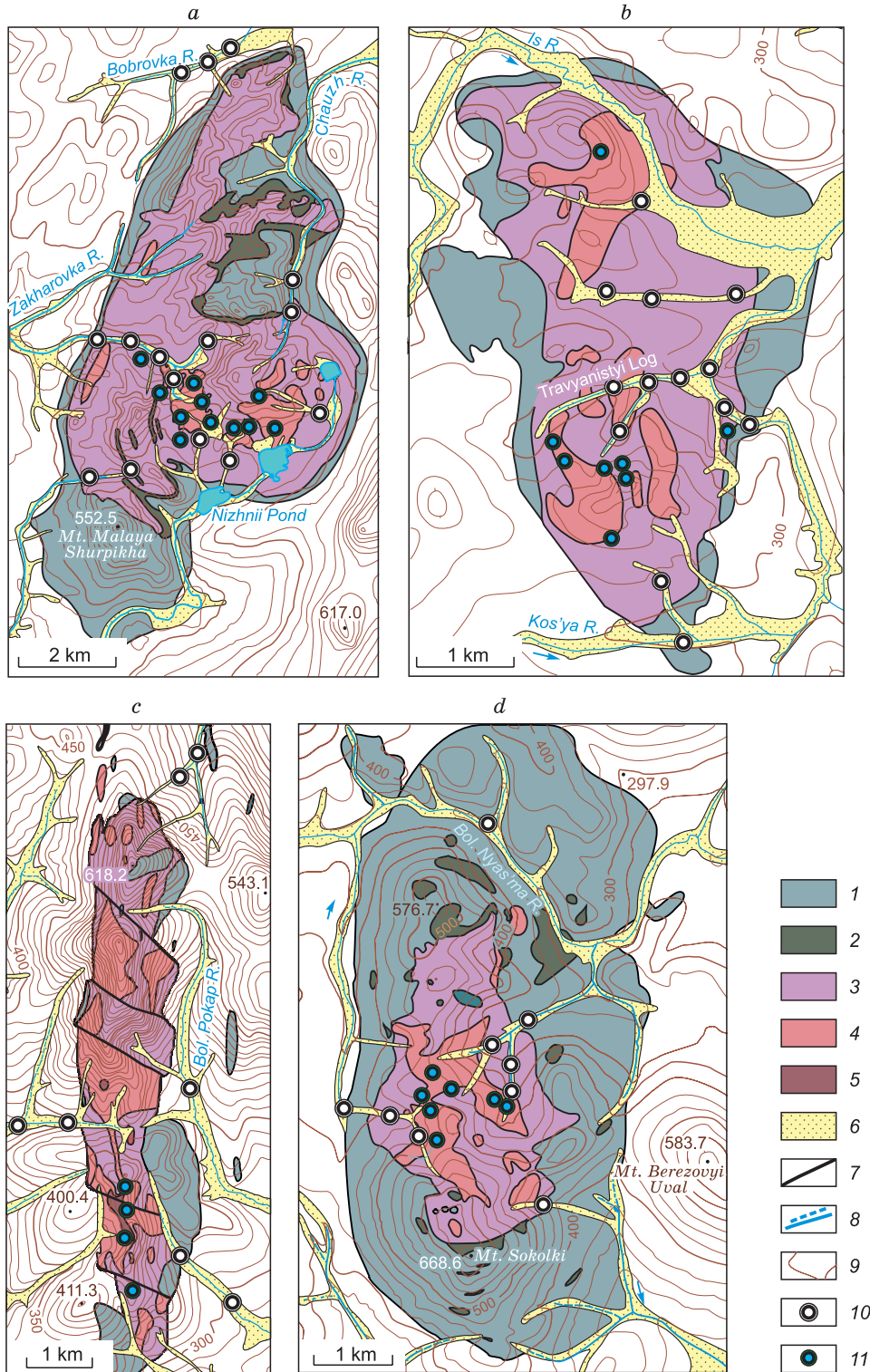
Fig. 1. Geological schemes of clinopyroxenite–dunite massifs of the Middle Urals, after Ivanov (1997), with major points of lump ore and bulk sampling. Massifs: *a*, Nizhnii Tagil, *b*, Svetlyi Bor, *c*, Veresovyi Bor, *d*, Kamenushenskii. *1*, pyroxenites; *2*, wehrlites; *3–5*, dunites: *3*, fine- and medium-grained, *4*, medium- and coarse-grained, *5*, coarse-grained and pegmatoid; *6*, alluvial and technogenic deposits; *7*, faults; *8*, hydrographic network; *9*, surface contours; *10*, points of sampling at placers; *11*, points of sampling of bedrocks.

Ray Diffraction Methods of Research" Resource Center of the Scientific Park of St. Petersburg State University. Qualitative X-ray phase analysis was performed by the Gandolfi method on a Rigaku R-AXIS RAPID II single-crystal diffractometer with a cylindrical detector ($d = 127.4$ mm; CoK_α radiation), followed by the processing of the obtained X-ray powder patterns by the OSC2XRD (Britvin et al., 2017) and PDXL-2 (analyst A.A. Zolotarev, Jr.) software.

PLATINUM-GROUP MINERALS

The main specifics of platinum-group mineralization of zoned clinopyroxenite–dunite massifs in the Middle Urals is a predominance of Pt–Fe alloys among platinum-group minerals (Lazarenkov et al., 1992; Ivanov, 1997). According to the proposed classification of Pt–Fe alloys (Cabri and Feather, 1975), ferroplatinum (space group *Fm3m*, Fe = 20–50 at.%) cannot be distinguished from isoferroplatinum (space group *Pm3m*, Fe = 25–35 at.%) only on the basis of their chemical compositions. Using X-ray phase analysis data, it was established that ferroplatinum with a bulk-centered cell (*Fm3m*) dominates over isoferroplatinum with a primitive cell (*Pm3m*) among Pt–Fe minerals of chromitites and placers of the Nizhnii Tagil massif (Fig. 2*a*, *e*), which agrees with the results of previous studies (Malitch and Thalhammer, 2002). Most of Pt–Fe minerals from chromitites and placers of the Svetlyi Bor (Fig. 2*b*, *f*), Veresovyi Bor (Fig. 2*c*, *g*), and Kamenushenskii (Fig. 2*d*, *h*) massifs, including those similar in composition to Pt_2Fe, have a primitive cell (*Pm3m*), which permits them to be referred to as isoferroplatinum. The chemical composition of most of

the studied isoferroplatinum grains from the Svetlyi Bor massif is close to Pt_3Fe. A specific feature of Pt–Fe minerals from chromitites and placers of the Nizhnii Tagil massif is the abundance of Pt–Fe alloy compositionally similar to Pt_2Fe. According to X-ray phase analysis, the rocks of the Veresovyi Bor massif contain only isoferroplatinum; in primary chromitites it has composition Pt_3Fe, and in placers associated with the massif, its composition varies from Pt_3Fe to Pt_2Fe.

Minerals of the tetraferroplatinum group were found in chromitites and placers of all the studied massifs, but they are most widespread is the Nizhnii Tagil (Fig. 3*a*, *e*) and Veresovyi Bor (Fig. 3*c*, *g*) massifs. Minerals of intermediate composition of the series tulameenite–ferronickelplatinum are predominant in chromitites of the Nizhnii Tagil massif. Tulameenite and tetraferroplatinum prevail in the Veresovyi Bor massif; they form rims over isoferroplatinum grains. Estimating the contents of tulameenite, tetraferroplatinum, and ferronickelplatinum in placers, we should note that they are abundant only in eluvial, deluvial, and ravine placers. The contents of these minerals regularly decrease with distance from the primary source, which was established during the study of PGE from the placers of the Nizhnii Tagil (Stepanov et al., 2015) and Svetlyi Bor (Stepanov et al., 2019) massifs.

Minerals of the tetraferroplatinum group are seldom found in chromitites and placers of the Svetlyi Bor (Fig. 3*b*, *f*) and Kamenushenskii (Fig. 3*d*, *h*) massifs, whereas dunites of the Svetlyi Bor massif contain an almost complete isomorphic series $PtFe–Pt_2CuFe$ (Tolstykh et al., 2011). Tulameenite and tetraferroplatinum were found in this massif. Chromitites of the Kamenushenskii massif contain minerals of intermediate
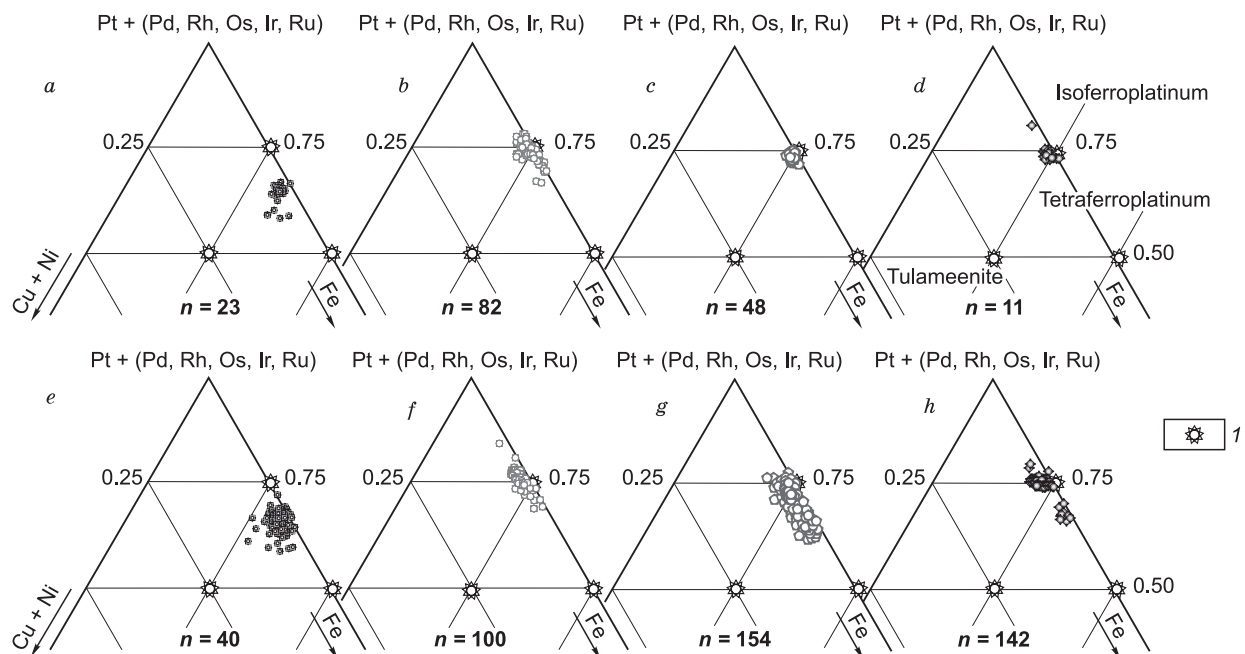

Fig. 2. Composition diagrams for Pt–Fe alloys (at.%) from primary chromitites (*a–d*) and placers (*e–h*) of the Nizhnii Tagil (*a*, *e*), Svetlyi Bor (*b*, *f*), Veresovyi Bor (*c*, *g*), and Kamenushenskii (*d*, *h*) massifs. *N*, number of analyses, *1*, points corresponding to the ideal compositions of the minerals.
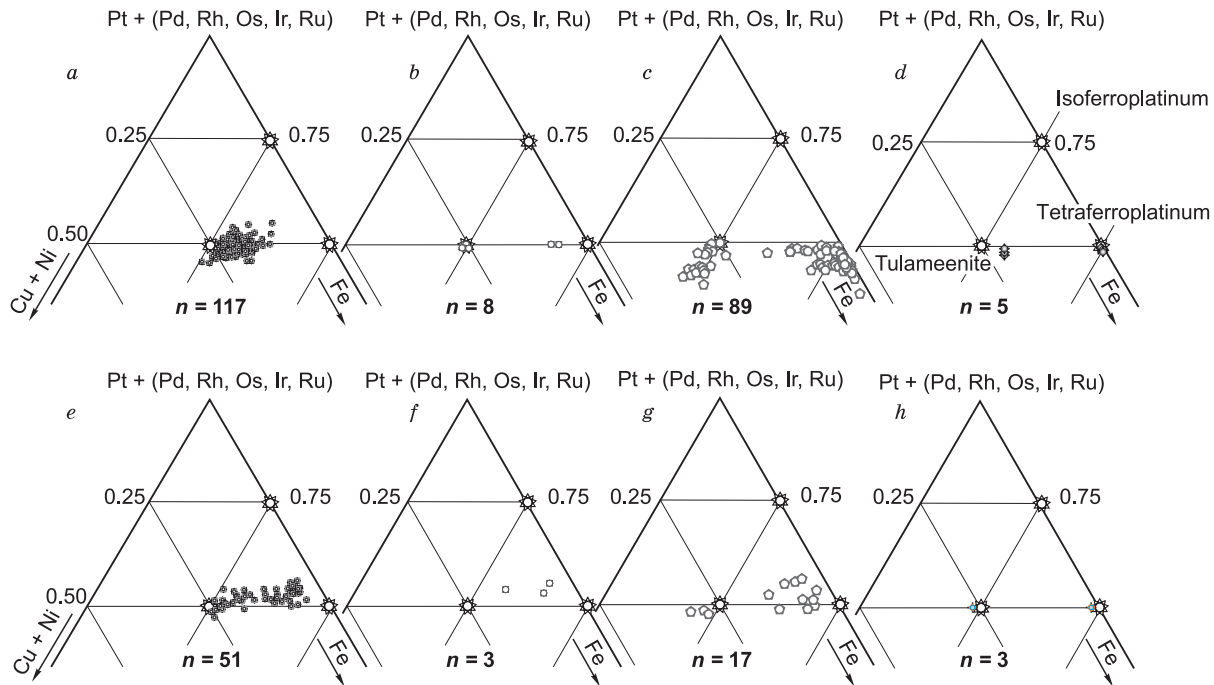
Fig. 3. Composition diagrams for tetraferroplatinum group minerals (at.%) from chromitites (*a–d*) and placers (*e–h*). For explanation, see Fig. 2.

composition of the isomorphic series tulameenite–tetraferroplatinum, with a predominance of tulameenite.

In the PGE–Fe–(Ni + Cu) diagrams for platinum-group minerals from chromitites and placers of the Nizhnii Tagil massif (Fig. 3), one can see a distinct single composition field between the compositions of tetraferroplatinum and tulameenite. Within this field, there are analytical points corresponding to ferronickelplatinum and tulameenite, which is seen in the Fe–Cu–Ni plot (Fig. 4). The abundance of ferronickelplatinum is a specific feature of the Nizhnii Tagil massif, distinguishing it from the other Middle Urals clinopyroxenite–dunite massifs with prevailing intermediate minerals of the series tulameenite–tetraferroplatinum.

A wide range of platinum-group mineral inclusions is identified in Fe–Pt minerals. In Pt–Fe alloys from chromitites and placers of the Svetlyi Bor massif, impurities of Ru–Os sulfides of the series laurite–erlichmanite (Fig. 5*a*, *d*), Ir–Rh sulfides of the series kashinite (Ir_2S_3)–bowieite (Rh_2S_3) (Fig. 5*b*, *e*), and Ir–Rh–Pt thiospinels of the series cuproiridsite ($CuIr_2S_4$)–cuprorhodsite ($CuRh_2S_4$)–malanite ($CuPt_2S_4$) are predominant. Sulfides of Rh and Ir are found only in Pt minerals from chromitites of the Svetlyi Bor, Veresovyi Bor, and Kamenushenskii massifs. The Pt–Fe minerals from all the studied massifs abound in Os–Ir–Ru alloys (Fig. 5*c*, *f*). According to the nomenclature by Harris and Cabri (1991), the studied Os–Ir–Ru alloys are osmium and iridium. The Pt–Fe minerals of the Veresovyi Bor and Kamenushenskii massifs contain numerous tabular osmium inclusions. The Os–Ir–Ru alloys of the Nizhnii Tagil massif are osmium with a high content of iridium or iridium with a

high content of osmium. The chromitites of the Svetlyi Bor massif contain grains and aggregates of iridium; the latter was also found as inclusions in Pt–Fe minerals, along with osmium inclusions. A specific feature of the inclusions in isoferroplatinum of the Kamenushenskii massif is the abun-
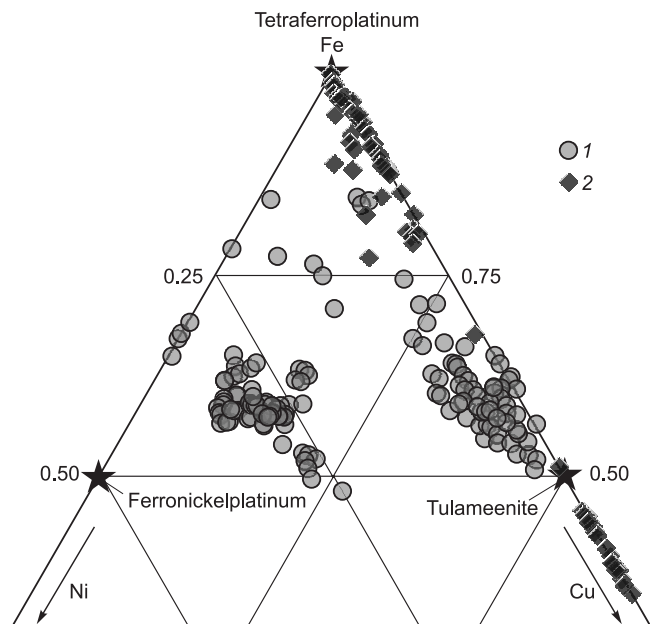

Fig. 4. Cu–Ni–Fe composition diagrams for tetraferroplatinum group minerals (at.%) from chromitites of the Nizhnii Tagil (*1*) and Veresovyi Bor (*2*) massifs. Asterisks mark the points of the ideal compositions of minerals.
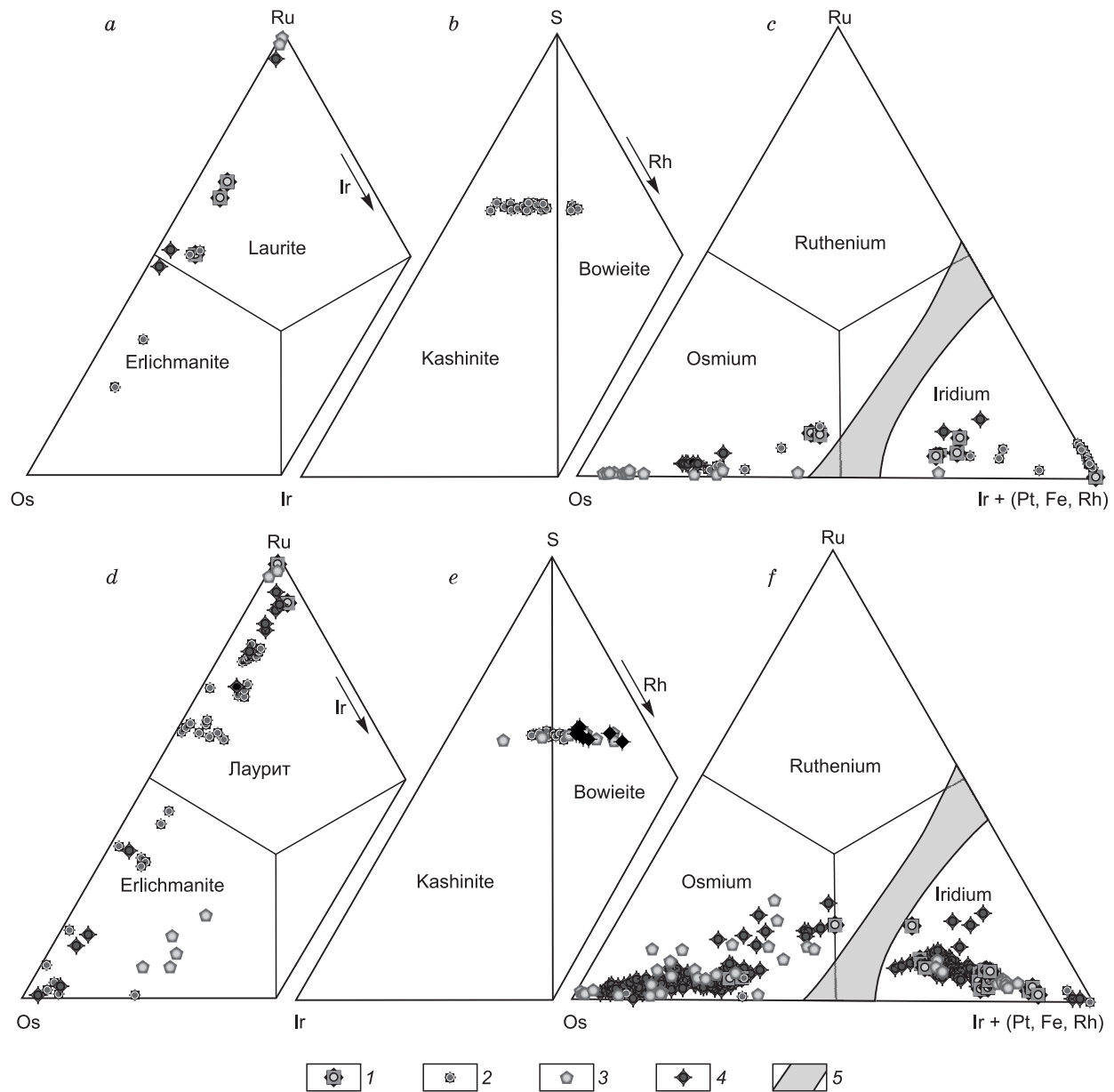
Fig. 5. Composition diagrams for mineral inclusions (at.%) in the Pt–Fe matrix from chromitites (*a–c*) and placers (*d–f*) of the massifs: *1*, Nizhnii Tagil (*n* = 11/24); *2*, Svetlyi Bor (*n* = 63/51), *3*, Veresovyi Bor (*n* = 17/52), *4*, Kamenushenskii (*n* = 17/123), *5*, immiscibility gap. *n*, number of analyses (chromitites/placers).

dance of both hexagonal osmium plates and isometric iridium segregations.

The latest platinum-group minerals are sulfides, sulfoantimonides, sulfoarsenides, plumbides, and tellurides. Irarsite and hollingworthite are developed as secondary minerals after primary Pt–Fe intermetallic compounds of the Nizhnii Tagil and Kamenushenskii massifs. Ferhodsite occurs among platinum-group minerals of the Nizhnii Tagil and Veresovyi Bor massifs (Begizov and Zav'yalov, 2016). The platinum-group mineral assemblage of the Veresovyi Bor massif includes abundant secondary minerals, such as irarsite, hollingworthite, potarite, plumbopalladinite, cooperite,

rhodplumsite, zvyagintsevite, unnamed telluride phases (Pb, Bi) Rh_2Te_3, and an unnamed mineral Cd–Hg–Pd (Stepanov et al., 2018).

MORPHOLOGICAL FEATURES OF GRAINS AND AGGREGATES OF PLATINUM-GROUP MINERALS

We analyzed the forms and internal structure of platinum-group minerals from primary sources and placers located not far from the massifs in which grains and aggregates of platinum-group minerals were treated by natural processes. As noted above, Pt–Fe minerals are predominant
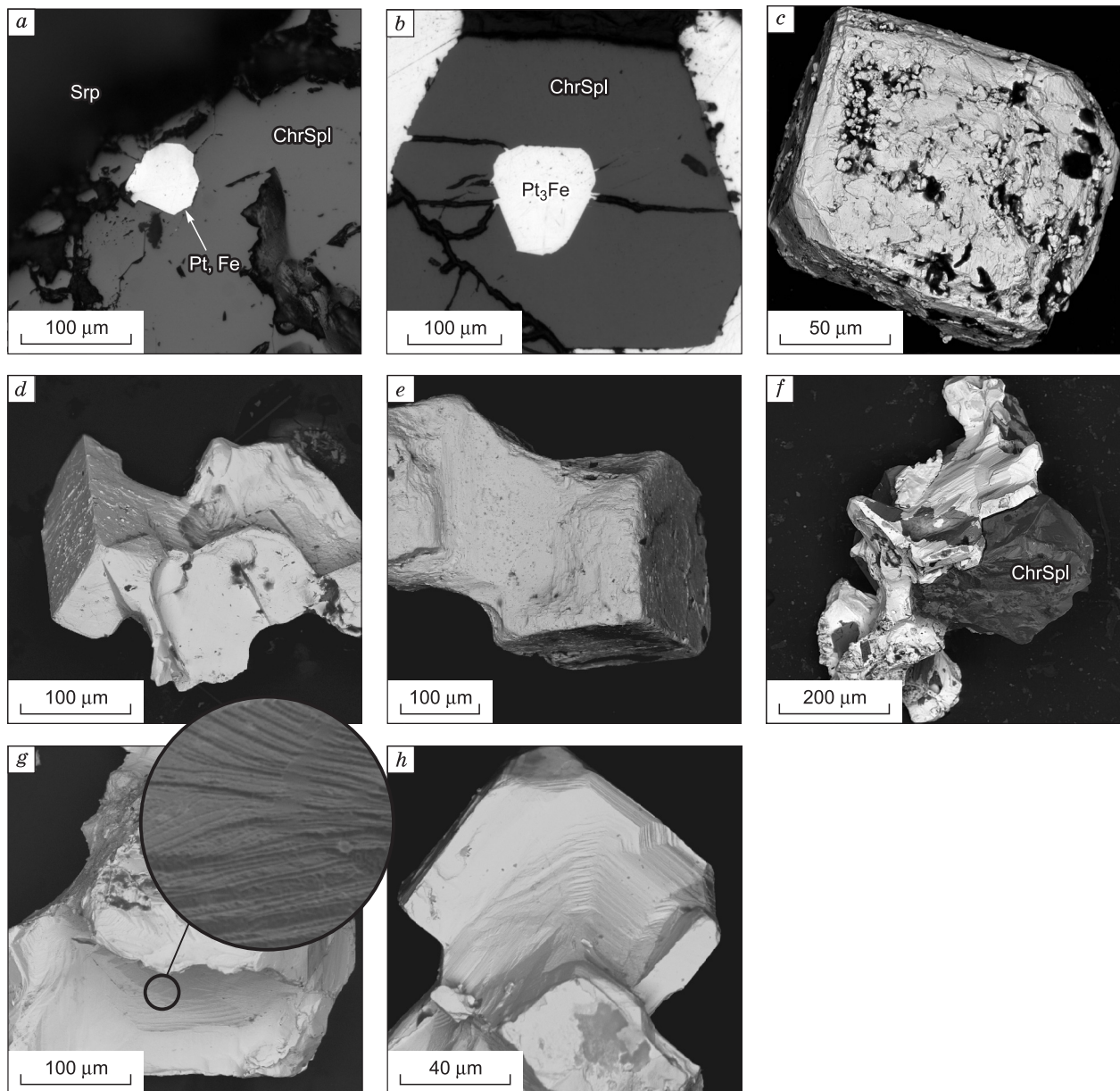
Fig. 6. Morphology of Pt–Fe minerals from chromitites of the Nizhnii Tagil (*a*, *c*), Veresovyi Bor (*b*, *e*, *f*, *g*), Svetlyi Bor (*d*), and Kamenushenskii (*h*) massifs. Hereafter, Pt₃Fe, mineral compositionally corresponding to isoferroplatinum; Pt, Fe, mineral compositionally corresponding to ferroplatinum; CrSpl, Cr-spinel, Srp, serpentine. SEM images (BSE mode).

among all platinum-group minerals. Isoferroplatinum is found as inclusions in Cr-spinel crystals and as individual faceted crystals and complex granular masses "cementing" Cr-spinel aggregates. Inclusions of Pt–Fe minerals in Cr-spinel (Fig. 6*a*, *b*) are faceted mostly to a simple crystal form, but the orientation of isoferroplatinum grains relative to Cr-spinel crystals in some samples permits considering these faceted inclusions to be a negative crystal (Fig. 6*b*) in Cr-spinel. The inclusions are no larger than 100 μm. Crystals of Pt–Fe minerals are extremely rare and measure, on the average, 150–200 μm. All the crystals are of cubic habit (Fig. 6*c*, *d*, *h*), which distinguishes chromite–platinum min-

eralization from dunite one characterized by not only cubic but also cuboctahedral mineral crystals (Tolstykh et al., 2011). Seldom, in addition to the cube face {100}, the faceted crystals of Pt–Fe minerals have rhombododecahedron face {110} and octahedron face {111} (Fig. 6*c*). There are also occasional fluorite-type intergrowths of isoferroplatinum (Fig. 6*d*). Most aggregates of Pt–Fe minerals vary in size from 0.5 mm to 5–6 cm; the largest of them are typical of the Nizhnii Tagil and Veresovyi Bor massifs (Zavaritskii, 1928; Betekhtin, 1935; Trushin et al., 2017). These aggregates "cement" individual Cr-spinel grains to form xenomorphic (to a first approximation) surfaces (Fig. 6*f*). A detailed
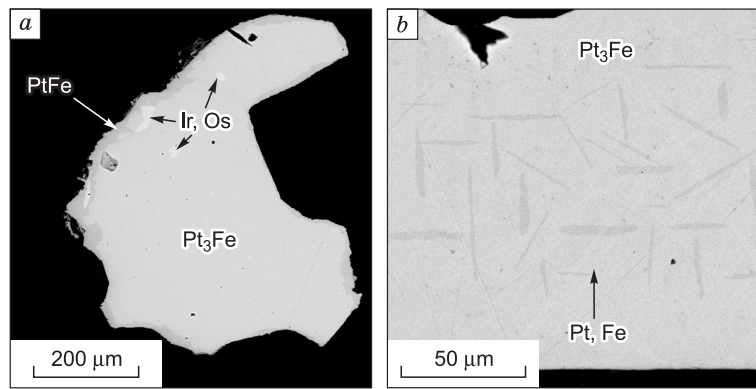
Fig. 7. Internal structure of Pt–Fe mineral crystals from chromitites of the Nizhnii Tagil (*a*) and Veresovyi Bor (*b*) massifs. Hereafter, PtFe, tetraferroplatinum; Ir, Os, iridium. SEM images (BSE mode).

study of the contacts between Cr-spinel and isoferroplatinum grains has revealed induction surfaces formed during their co-growth (Fig. 6*g*). Betekhtin (1935) regarded cubic isoferroplatinum grains in Cr-spinel as metacrysts, but the combination of growth habits with co-growth surfaces in their faceting (Fig. 6*h*) indicates simultaneous crystallization of Pt–Fe mineral and Cr-spinel.

Most of the individual grains of primary Pt–Fe alloys have a homogeneous internal structure without a distinct chemical zoning (Fig. 7*a*). Some grains have a structure formed, probably, during the successive crystallization of Pt–Fe alloy similar in composition to Pt_2Fe and, then, of isoferroplatinum (Fig. 7*b*).

Pt–Fe minerals from chromitites of the Middle Urals clinopyroxenite–dunite massifs contain mostly inclusions of Os–Ir–(Ru) alloys. In general, osmium is abundant in Pt–Fe minerals from chromitites of the Veresovyi Bor and Kamenushenskii massifs, is scarce in isoferroplatinum of the Svetlyi Bor massif, and is extremely rare in Pt–Fe minerals of the Nizhnii Tagil massif. Osmium occurs as euhedral crystals of pinacoidal habit (Fig. 8*a, b*) of different sizes, but the tabular crystals are seldom longer than 200 μm at the pinacoid face and are 10–15 μm in thickness. There are occa-

sional inclusions of euhedral pinacoidal osmium crystals in Cr-spinel intergrown with Pt–Fe minerals (Fig. 8*c*). Tabular osmium crystals are often localized at the phase boundary between Cr-spinel and ferroplatinum (Fig. 8*d*) or are present both in the Cr-spinel crystal and in the Pt–Fe matrix (Fig. 8*e*). In general, the osmium grains are unzoned. However, the contents of Ir and other PGE vary significantly within the tabular osmium crystals intergrown with granular iridium aggregates (Table 1; Fig. 8*h*). The morphology of the osmium plates and their genetic relations with the other minerals suggest that osmium was the first to crystallize.

Iridium inclusions are abundant in Pt–Fe minerals of the Nizhnii Tagil, Svetlyi Bor, and Kamenushenskii massifs. The inclusions in isoferroplatinum are of diverse morphology. Iridium segregations overgrowing Cr-spinel (Fig. 9*a*) or osmium plates (Figs. 8*h* and 9*b*), are rare. They contain products of breakdown of Pt–Fe–Ir alloy, with fine isometric isoferroplatinum grains (Ramdohr, 1969). These morphologic features indicate that part of iridium grains formed after osmium before the crystallization of the bulk of Pt–Fe alloys. There are numerous products of breakdown of solid solution of iridium in isoferroplatinum, with disseminated emulsion of fine isometric iridium grains in the Pt–Fe matrix

Table 1. Chemical composition of inclusions of Os–Ir–Ru intermetallic compounds in Pt–Fe minerals from chromitites and placers of the Nizhnii Tagil (1), Svetlyi Bor (2), Veresovyi Bor (3, 4), and Kamenushenskii (5–8) massifs (wt.%)

No.	Fe	Ru	Rh	Os	Ir	Pt	Σ	Formula
1	1.21	5.80	–	53.80	39.20	–	100.00	$Os_{0.50}Ir_{0.36}Ru_{0.10}Fe_{0.04}$
2	0.21	0.95	–	68.10	30.90	–	100.20	$Os_{0.67}Ir_{0.30}Ru_{0.02}Fe_{0.01}$
3	0.13	0.23	–	94.60	6.01	–	100.90	$Os_{0.93}Ir_{0.06}$
4	0.26	–	–	94.40	5.01	–	99.60	$Os_{0.94}Ir_{0.05}Fe_{0.01}$
5	0.18	8.82	2.02	48.22	39.92	–	99.16	$Os_{0.43}Ir_{0.36}Ru_{0.15}Rh_{0.03}Co_{0.01}$
6	0.34	2.64	1.04	65.49	29.18	0.37	99.06	$Os_{0.64}Ir_{0.28}Ru_{0.05}Rh_{0.02}Fe_{0.01}$
7	0.37	12.40	0.69	41.15	42.92	1.58	99.11	$Ir_{0.39}Os_{0.37}Ru_{0.21}Fe_{0.01}Rh_{0.01}Pt_{0.01}$
8	0.40	5.65	3.19	27.10	49.90	13.40	99.50	$Ir_{0.46}Os_{0.25}Pt_{0.12}Ru_{0.10}Rh_{0.05}Fe_{0.01}$

Note. The content of Co in analysis 5 is 0.61 wt.%. Analyses: 1–6, osmium, 7, 8, iridium. Hereafter, dash marks the content of element below its detection limit. Formulas are calculated per 100 at.%. The content of Pd is below its detection limit.
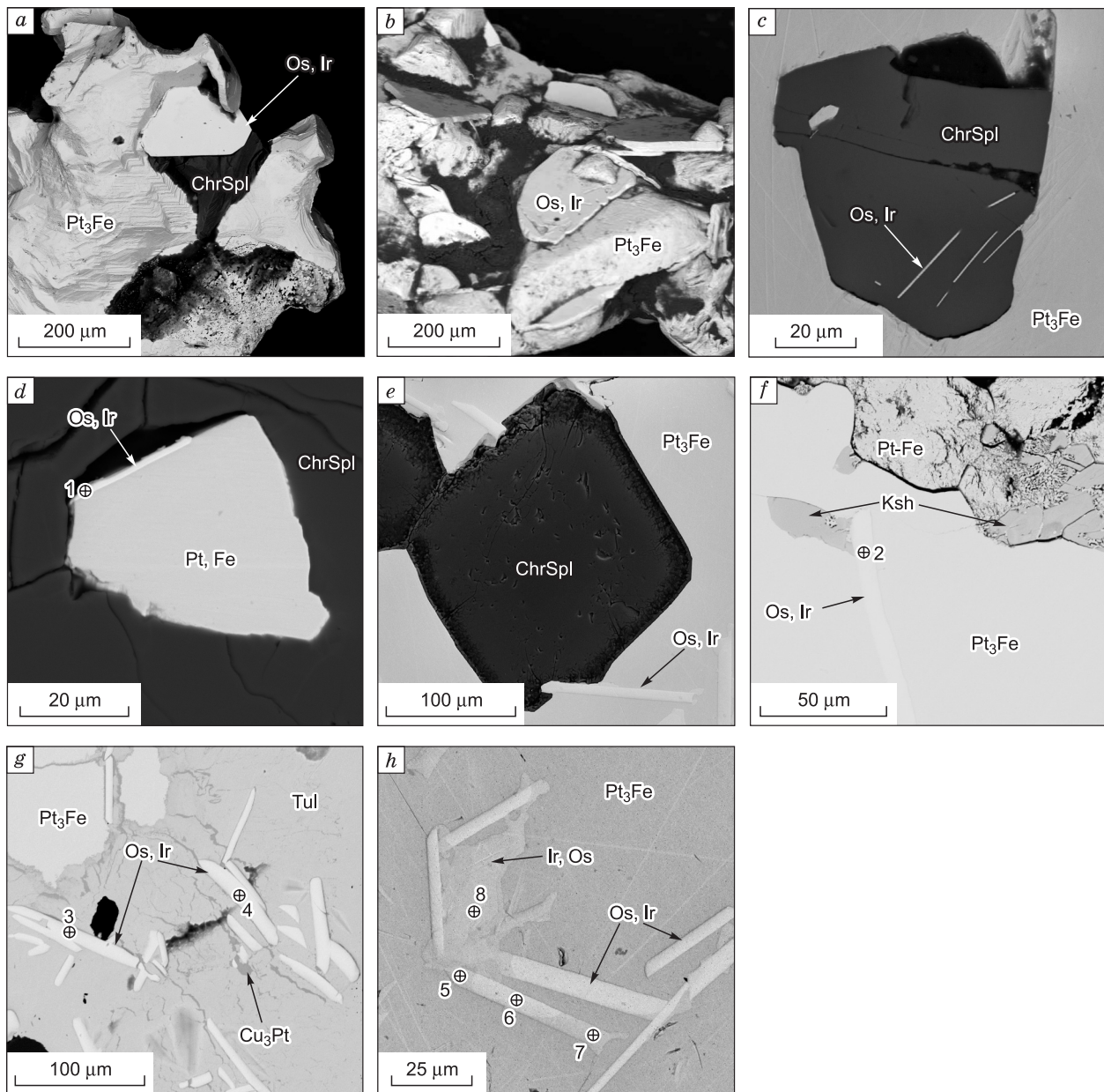
Fig. 8. Morphology and internal structure of osmium crystals in Pt–Fe minerals from chromitites and placers of the Svetlyi Bor (*a*, *f*), Kamenush-enskii (*b*, *e*, *h*), Veresovyi Bor (*c*, *g*), and Nizhnii Tagil (*d*) massifs. Pt–Fe, mixture of Fe–Pt minerals, Os, Ir, osmium, Ksh, kashinite, Tul, tula-meenite, Cu$_3$Pt, unnamed Cu–P mineral. Numbers of analytical points follow Table 1. SEM images (BSE mode).

prevailing (Fig. 9*c*). Coarser beam-shaped or tabular segre-gations of the breakdown products are scarcer. There is a complete series of intermediate products between the finely disseminated emulsion and tabular breakdown products (Fig. 9*d*). Isoferroplatinum enriched in disseminated iridium segregations has a high content of Ir (Table 2), whereas irid-ium is significantly enriched in Pt. Isoferroplatinum from chromitites of the Kamenushenskii, Svetlyi Bor, and, to a lesser extent, Nizhnii Tagil massifs contain inclusions of granular iridium aggregates, <1 mm in average size. Chro-mitites of the Svetlyi Bor massif contain iridium grains (Fig. 9*e*) and their aggregates up to several grams in weight

(Palamarchuk and Stepanov, 2016), which indicates ex-tremely high Ir enrichment of the mineral-forming medium.

Minerals of the isomorphic series laurite–erlichmanite are represented by two morphologic varieties. The first is single euhedral crystals localized on the margins of clusters of Pt–Fe minerals (Fig. 10*a*). Most of them have a distinct zoning with varying contents of Os and Ru (Table 3). The content of Os significantly increases toward to the marginal growth zones of crystals, up to the transition of laurite into erlichmanite. The second variety is laurite or erlichmanite crystals overgrowing Cr-spinel, probably with the formation of epitaxial intergrowths (Fig. 10*c*). Os–Ru sulfides are

Table 2. Chemical composition of iridium and accompanying Pt–Fe minerals from chromitites and placers of the Nizhnii Tagil (1, 2) and Svetlyi Bor (3–10) massifs (wt.%)

No.	Fe	Ni	Cu	Ru	Rh	Os	Ir	Pt	Σ	Formula
1	12.1	4.64	1.41	–	0.40	–	10.8	70.5	99.9	$(Pt_{0.98}Ir_{0.15}Rh_{0.01})_{1.14}(Fe_{0.59}Ni_{0.21}Cu_{0.06})_{0.86}$
2	9.72	3.44	0.58	0.72	1.36	–	23.5	61.1	100.3	$Pt_{0.45}Fe_{0.25}Ir_{0.18}Ni_{0.08}Rh_{0.02}Ru_{0.01}Cu_{0.01}$
3	7.94	–	1.01	–	0.55	–	3.57	86.3	99.3	$(Pt_{2.83}Ir_{0.12}Rh_{0.03})_{2.98}(Fe_{0.91}Cu_{0.10})_{1.01}$
4	8.22	–	1.05	–	–	–	3.14	87.6	99.9	$(Pt_{2.85}Ir_{0.10})_{2.95}(Fe_{0.94}Cu_{0.11})_{1.05}$
5	1.04	–	–	3.06	2.52	8.43	77.8	7.14	99.9	$Ir_{0.72}Os_{0.08}Pt_{0.07}Ru_{0.05}Rh_{0.04}Fe_{0.03}$
6	1.07	–	–	2.99	–	9.36	78.5	7.62	99.5	$Ir_{0.75}Os_{0.09}Pt_{0.07}Ru_{0.05}Fe_{0.04}$
7	0.77	–	–	1.97	2.56	–	83.6	11.1	100.0	$Ir_{0.79}Pt_{0.10}Rh_{0.05}Ru_{0.04}Fe_{0.03}$
8	0.60	–	0.28	1.52	2.16	–	83.4	11.3	99.2	$Ir_{0.80}Pt_{0.11}Rh_{0.04}Ru_{0.03}Fe_{0.02}Cu_{0.01}$
9	0.80	–	–	1.52	2.44	–	81.8	13.4	99.9	$Ir_{0.78}Pt_{0.13}Rh_{0.04}Ru_{0.03}Fe_{0.03}$
10	3.35	–	0.28	1.10	1.57	–	44.7	48.9	100.0	$Pt_{0.44}Ir_{0.41}Fe_{0.10}Rh_{0.03}Ru_{0.02}Cu_{0.01}$

Note. Analyses: 1, Ir-containing tetraferroplatinum, the formula was calculated per two atoms; 2, ferroplatinum, the formula was calculated per 100%; 3, 4, isoferroplatinum, the formulas were calculated per four atoms; 5–9, Pt-containing iridium, the formulas were calculated per 100 at.%; 10, Ir–Pt alloy, the formula was calculated per 100%.

abundant in the platinum-group mineral assemblage from chromitites and placers of the Svetlyi Bor and Kamenushenskii massifs; however, the limited contents of laurite and erlichmanite are found in Pt–Fe minerals of other zoned massifs of the Middle Urals.

Minerals of the isomorphic series kashinite–bowieite are much scarcer in Pt–Fe minerals of the Middle Urals zoned massifs than laurite and erlichmanite. Like the above Os–Ru

sulfides, they are of two morphologic varieties: large (100–400 μm) segregations intergrown with Cr-spinel (Fig. 11*a*) and separate fine (<50 μm) euhedral crystals as inclusions in Pt–Fe minerals (Fig. 11*b*). Some inclusions of Rh and Ir sulfides have zoning caused by a predominance of the kashinite end-member in the crystal core and an increase in Rh content toward the marginal growth zones, up to the transition of kashinite into bowieite (Table 4, Fig. 11*b*). Locally, Os–
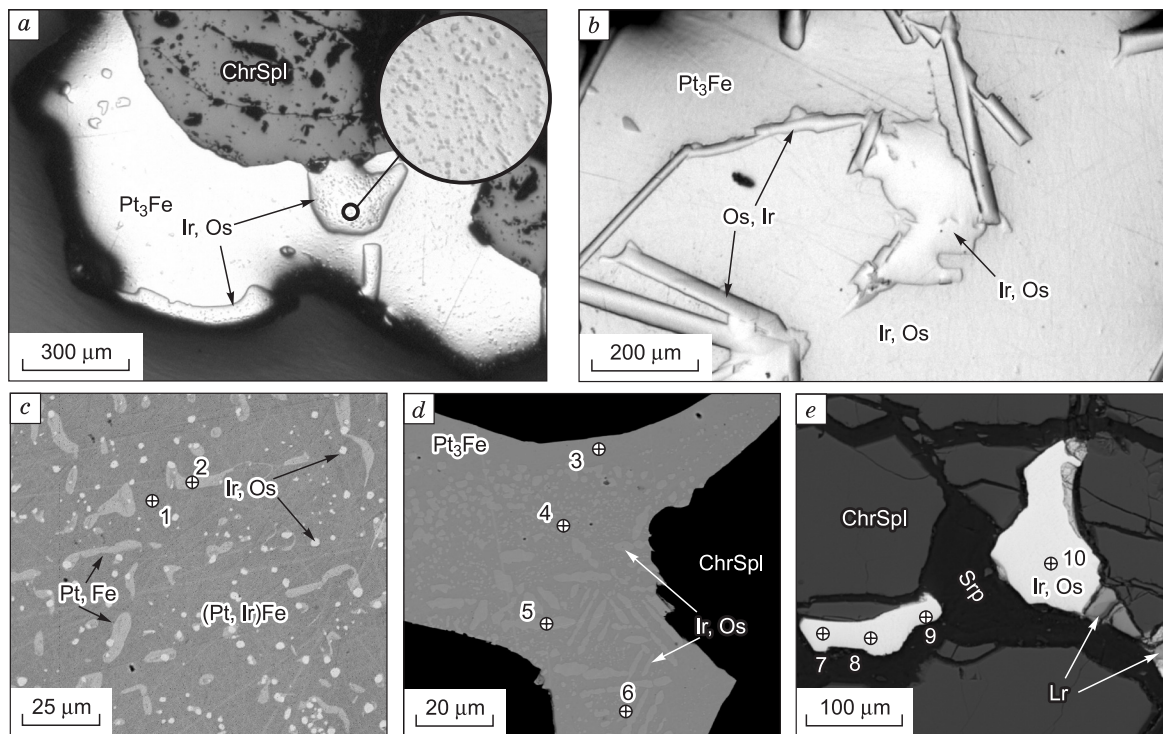

Fig. 9. Iridium inclusion in Pt–Fe minerals from chromitites and placers of the Kamenushenskii (*a*, *b*), Nizhnii Tagil (*c*), and Svetlyi Bor (*d*, *e*) massifs. Hereafter, (Pt, Ir)Fe, Ir-containing tetraferroplatinum, Lr, laurite. Numbers of analytical points follow Table 2. Reflected-light (*a*, *b*) and SEM (BSE mode) (*c–e*) images. *a*, Breakdown of solid solution of iridium in isoferroplatinum and of Pt–Fe mineral in iridium. *c*, *d*, Different products of breakdown of solid solution of iridium in isoferroplatinum.
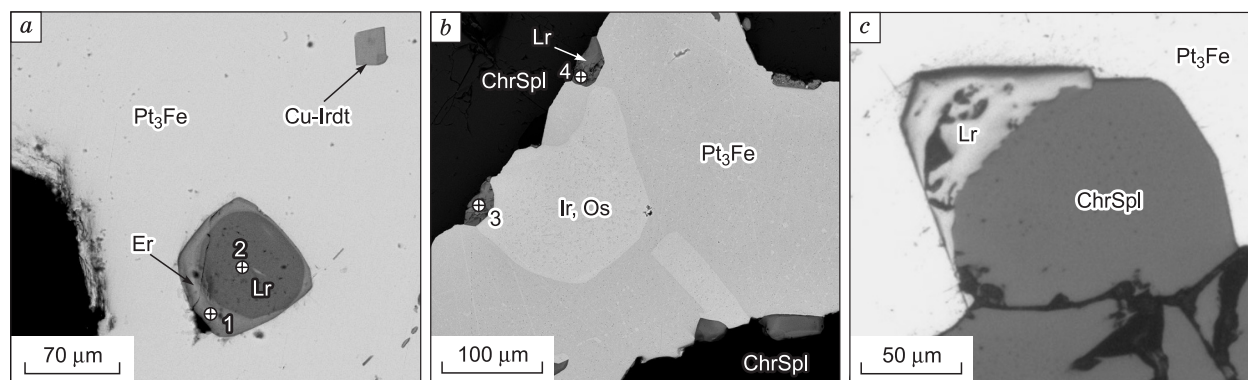
Fig. 10. Inclusions of minerals of the isomorphous series laurite–erlichmanite in Pt–Fe minerals from chromitites and placers of the Svetlyi Bor (*a*), Kamenushenskii (*b*), and Veresovyi Bor (*c*) massifs. Hereafter, Er, erlichmanite, Cu–Irdt, cuproiridsite. Numbers of analytical points follow Table 3. SEM (BSE mode) (*a*, *b*) and reflected-light (*c*) images. *b*, Fine spot breakdown of Pt–Fe mineral in iridium.

Ir–Ru alloys are replaced by kashinite (Fig. 11*c*). Kashinite and bowieite were found as inclusions in Pt–Fe alloys of the Svetlyi Bor, Veresovyi Bor, and Kamenushenskii (single findings) massifs but not revealed in platinum-group minerals from chromitites of the Nizhnii Tagil massif. There are also intergrowths of kashinite with Ir–Rh thiospinels (Fig. 11*d*; Table 4). Ir–Rh thiospinels of the series ferrorhodsite–cuprorhodsite–cuproiridsite are typomorphic in-clusions in Pt–Fe minerals from zoned massifs (Podlipskii et al., 1999) but are scarce inclusions in Pt–Fe alloys from chromitites of the Middle Urals clinopyroxenite–dunite massifs. They are present in high contents in Pt–Fe minerals of the Svetlyi Bor and Veresovyi Bor massifs. Single inclu-sions of cuproiridsite were found in isoferroplatinum from chromitites of the Kamenushenskii massif. Minerals of the series ferrorhodsite–cuprorhodsite are usually present as

Table 3. Chemical composition of laurite and erlichmanite from chromitites and placers of the Svetlyi Bor (1, 2) and Kamenushenskii (3, 4) massifs (wt.%)

No.	Ru	Rh	Os	Ir	Pt	S	Σ	Formula
1	18.7	–	47.6	5.65	–	28.0	99.9	$(Os_{0.56}Ru_{0.42}Ir_{0.07})_{1.05}S_{1.95}$
2	34.9	–	29.9	3.74	–	31.3	99.9	$(Ru_{0.69}Os_{0.32}Ir_{0.04})_{1.05}S_{1.95}$
3	36.1	0.67	21.8	8.01	–	34.6	101.1	$(Ru_{0.68}Os_{0.21}Ir_{0.08}Rh_{0.01})_{0.98}S_{2.02}$
4	29.2	0.58	29.1	8.80	0.61	32.9	101.1	$(Ru_{0.57}Os_{0.30}Ir_{0.09}Pt_{0.01})_{0.97}S_{2.02}$

Note. 1, erlichmanite; 2–4, laurite, the formulas were calculated per three atoms.

Table 4. Chemical composition of laurite, kashinite, bowieite, and Ir–Rh thiospinels from chromitites and placers of the Svetlyi Bor (1, 2, 7–10, 12), Veresovyi Bor (5, 6), and Kamenushenskii (3, 4) massifs, wt.%

No.	Fe	Cu	Ru	Rh	Os	Ir	Pt	S	Σ	Formula
1	–	0.18	35.1	1.36	22.1	6.29	0.30	34.7	100.1	$(Ru_{0.65}Os_{0.22}Ir_{0.06}Rh_{0.02}Cu_{0.01})_{0.96}S_{2.03}$
2	–	–	–	23.9	–	50.7	–	25.4	100.1	$(Ir_{1.02}Rh_{0.90})_{1.93}S_{3.07}$
3	–	–	–	34.8	–	38.8	–	27.4	100.9	$(Rh_{1.21}Ir_{0.73})_{1.94}S_{3.06}$
4	–	–	–	47.4	–	23.9	–	28.8	100.2	$(Rh_{1.51}Ir_{0.42})_{1.98}S_{3.02}$
5	–	–	–	14.4	–	62.4	–	22.9	100.6	$(Ir_{1.38}Rh_{0.59})_{1.97}S_{3.03}$
6	–	–	–	26.2	–	51.0	–	22.6	100.6	$(Ir_{1.08}Rh_{1.04})_{2.12}S_{2.88}$
7	5.56	5.18	–	30.5	–	34.9	–	25.7	101.8	$(Fe_{0.48}Cu_{0.39})_{0.87}(Rh_{1.42}Ir_{0.87})_{2.29}S_{3.84}$
8	5.23	6.06	0.11	13.6	0.19	50.7	–	25.6	101.6	$(Cu_{0.48}Fe_{0.47})_{0.96}(Ir_{1.33}Rh_{0.67})_{2.00}S_{4.03}$
9	0.99	–	–	22.2	–	52.6	0.29	23.7	99.8	$(Ir_{1.10}Rh_{0.87}Fe_{0.07}Pt_{0.01})_{2.05}S_{2.96}$
10	0.82	0.62	–	20.3	–	53.2	0.37	22.9	98.3	$(Ir_{1.14}Rh_{0.81}Fe_{0.06}Cu_{0.04}Pt_{0.01})_{2.06}S_{2.94}$
11	7.49	7.34	0.24	44.2	0.22	9.20	1.96	29.6	100.2	$(Fe_{0.57}Cu_{0.49})_{1.06}(Rh_{1.81}Ir_{0.20}Pt_{0.04}Ru_{0.01})_{2.06}S_{3.88}$
12	0.27	11.01	–	10.9	–	39.3	13.46	24.6	100.1	$(Cu_{0.91}Ni_{0.05}Fe_{0.03})_{0.99}(Ir_{1.07}Rh_{0.56}Pt_{0.36})_{1.99}S_{4.02}$

Note. The content of Ni in an. 12 is 0.52 wt.%. 1, laurite, the formula was calculated per three atoms; 2, 5, 6, 9, 10, kashinite, 3, 4, bowieite, the formulas were calculated per five atoms; 7, 11, ferrorhodsite, 8, 12, cuproiridsite, the formulas were calculated per seven atoms.
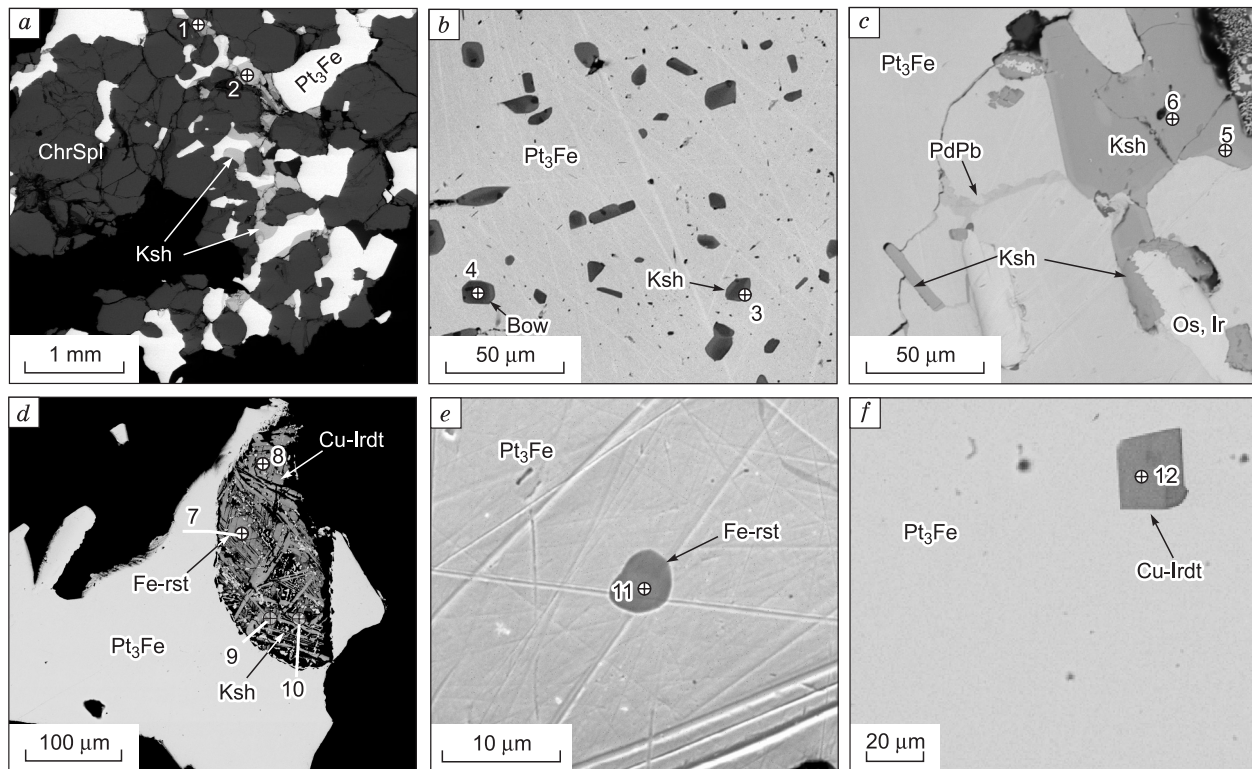
Fig. 11. Inclusions of PGE sulfides and Ir–Rh thiospinels in isoferroplatinum from chromitites of the Svetlyi Bor (*a*, *d*, *f*), Kamenushenskii (*b*), and Veresovyi Bor (*c*, *e*) massifs. Hereafter, Fe-rst, ferrorhodsite, PdPb, zvyagentsevite, PdHg, potarite, Bow, bowieite. Numbers of analytical points follow Table 4. SEM (BSE mode) images.

euhedral crystals or isometric grains smaller than 100 µm in the Pt–Fe matrix (Fig. 11*e*, *f*). The composition of these minerals is given in Table 4. There are also extremely rare large (>100 µm) isometric segregations confined to the edges of Pt–Fe alloy grains (Stepanov et al., 2017).

Most of the grains of Pt–Fe alloys from chromitites and placers of the Nizhnii Tagil and Veresovyi Bor massifs, corresponding in composition to ferroplatinum or isoferroplatinum, are replaced by late secondary minerals of the tetraferroplatinum group. However, the formation of new minerals was preceded by a serious deformation of Pt–Fe minerals and inclusions in them. Osmium and Cr-spinel were subjected mostly to brittle deformations. Tabular osmium segregations are often broken or cracked at the site of bending (Fig. 12*a*, *b*); more seldom, they are bent without brittle deformation (Fig. 12*c*). Ductile Pt–Fe minerals undergo plastic deformations and are often "pressed" into extension fractures in osmium crystals and into the interstices of Cr-spinel aggregate (Fig. 12*d*–*f*). These transformations of minerals occurred, probably, at high stress and temperatures significantly lower than their melting temperatures.

After plastic deformations, aggregates and grains of Pt–Fe minerals were replaced by secondary minerals of the tetraferroplatinum group. In most cases, these minerals formed rims with preserved relics of primary composition (Fig. 13*a*). In some isoferroplatinum grains, the front of metasomatic

replacement by tetraferroplatinum or tulameenite is related to the spread of deformation structures (Fig. 13*b*) along (111) corresponding to cleavage (Betekhtin, 1935; Tolstykh et al., 2015). The grains of Pt–Fe minerals show different degrees of replacement of primary Pt–Fe minerals along cleavage cracks and that along grain boundaries. In general, the development of tetraferroplatinum group minerals along cleavage cracks in Pt–Fe minerals is the initial stage of their metasomatic transformation. Complete pseudomorphs of tetraferroplatinum group minerals developed after primary Pt–Fe minerals are the final product of these transformations. The replacement rims consist of numerous parallel elongate segregations distinct in the reflected light (when an optic analyzer is used) owing to the anisotropy of tetraferroplatinum group minerals (Fig. 13*c*). For chromitites of the Nizhnii Tagil massif it was established (Stepanov and Malich, 2016) that Pt–Fe alloys corresponding in composition to ferroplatinum are replaced by tulameenite and that Pt–Fe minerals with isoferroplatinum stoichiometry are replaced by ferronickelplatinum. In platinum-group minerals from chromitites of the Veresovyi Bor massif, Pt–Fe alloy compositionally similar to isoferroplatinum was replaced by tulameenite, and tulameenite, in turn, was replaced by tetraferroplatinum (Fig. 13*d*). Among Cu–Ni–Fe–PGE minerals, a mineral with Cu_3Pt stoichiometry pseudomorphically replacing tulameenite (Fig. 13*e*) or filling small cracks in it
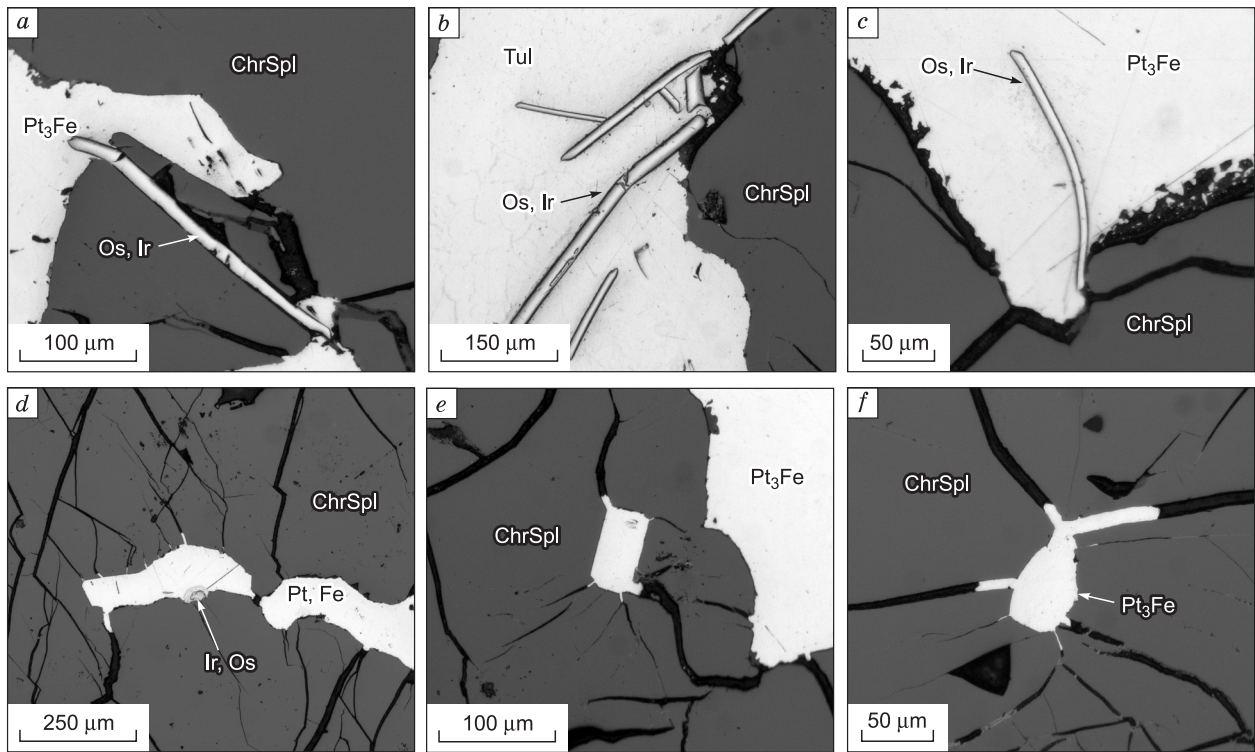
Fig. 12. Result of brittle deformation of Cr-spinel and Ir-containing osmium and plastic deformations of Pt–Fe minerals of the Veresovyi Bor (*a–c, e, f*) and Nizhnii Tagil (*d*) massifs. SEM (BSE mode) images.
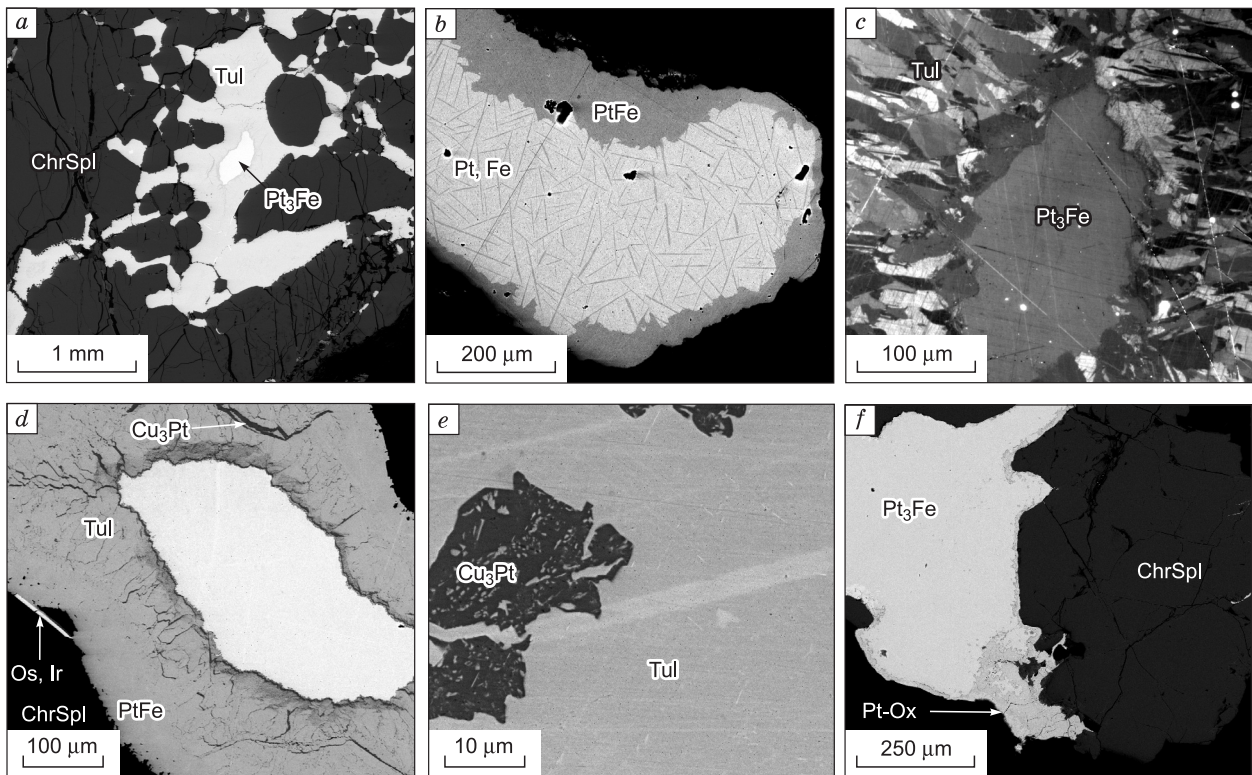

Fig. 13. Metasomatic aggregates of tetraferroplatinum group minerals replacing primary Pt–Fe minerals of the Veresovyi Bor (*a–d*) and Nizhnii Tagil (*e, f*) massifs. Pt–Ox, oxygen-containing platinum-group minerals. SEM (BSE mode) and reflected-light (with a microprobe) images (*c*).
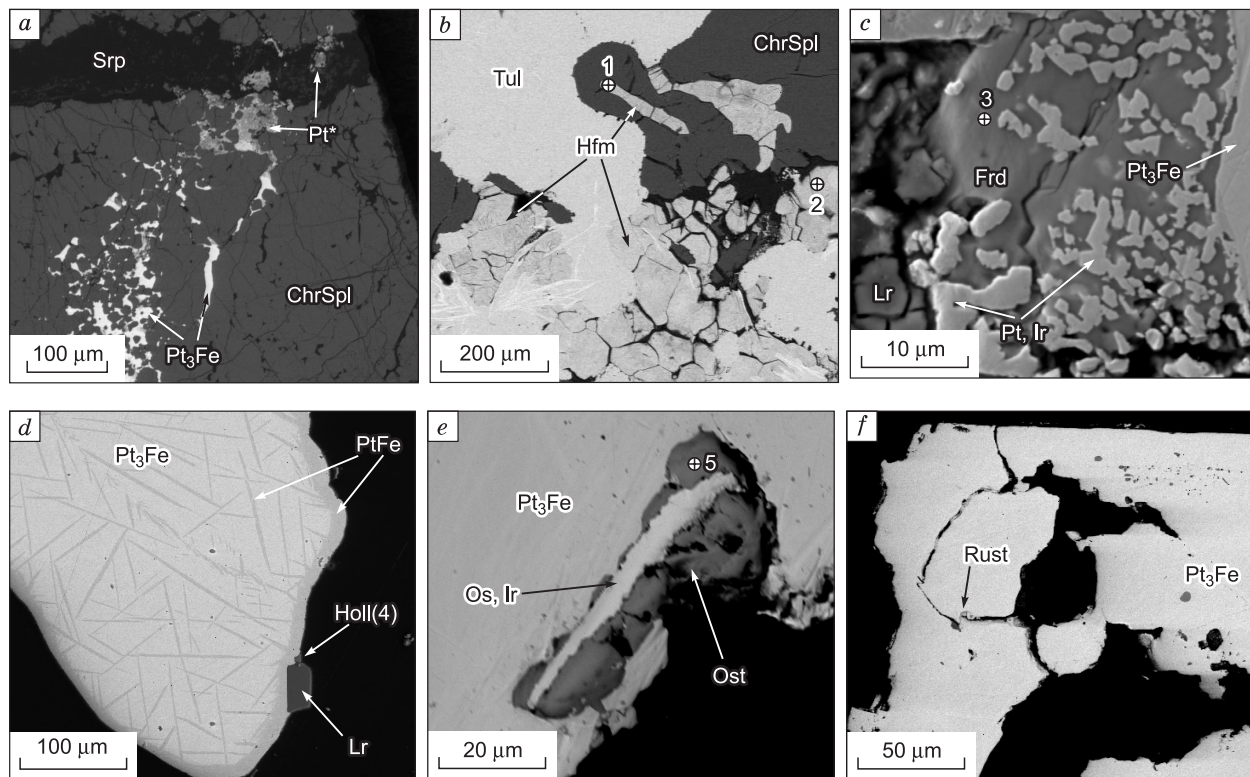
Fig. 14. Increase in the degree of alteration of Pt–Fe minerals on the approach to later formed serpentine veinlet in chromitities of the Veresovyi Bor massif (*a*); hexaferrum and PGE sulfides and sulfoarsenides of the late paragenesis from the Veresovyi Bor (*b*, *c*, *e*) and Nizhnii Tagil (*d*, *f*) massifs. Pt*, fine-crystalline aggregate of tetraferroplatinum and other minerals; Hfm, hexaferrum; PtS, cooperate; Po, pyrrhotite; Frd, ferhodsite; Pt, Ir, Ir-containing platinum; Holl, hollingworthite; Ost, osarsite; Rust, ruarsite. Numbers of analytical points follow Table 5. SEM (BSE mode) images.

was also found. Primary isoferroplatinum is seldom replaced by oxygen-containing platinum-group minerals (Fig. 13*f*).

Late serpentinization, expressed as the appearance of fine- to medium-tabular serpentine, led to active transformation of primary Pt–Fe alloys (Fig. 14*a*), inclusions in them, and tetraferroplatinum group minerals. Plates of Ir-containing osmium are replaced by hexaferrum, often with preserved primary crystallographic forms (Fig. 14*b*). Among PGE sulfides, minerals of the series kashinite–bowieite are most subjected to secondary transformations. They are replaced by a fine- and small-grained spongy aggregate of Pt–Fe minerals. Sulfides (cooperite and ferrodsite), arsenides (sperrylite), antimonides (stibiopalladinite) (Tolstykh et al., 2015), sulfoarsenides (irarsite, hollingworthite, osarsite, and ruarsite), sulfoantimonides (tolovkite), plumbides (zvyagintsevite and rhodplumsite), and amalgams (potarite) of PGE (Fig. 11*c*), seldom containing Te and Bi, were found in cracks and at the edges of Pt–Fe mineral grains. These minerals are especially widespread in Pt–Fe minerals from chromitites and placers of the Veresovyi Bor massif (Stepanov et al., 2018).

Ferhodsite is a PGE-containing structural analogue of pentlandite; it is more abundant than cooperite. This mineral in the form of complex aggregates containing numerous inclusions of Fe–Ir alloy replaces Pt–Fe intermetallic compounds of the Nizhnii Tagil (Begizov et al., 1976), Svetlyi

Bor (Stepanov, 2015), and Veresovyi Bor massifs (Fig. 14*c*). Inclusions of minerals of the series hollingworthite–irarsite were found in Pt–Fe minerals from chromitites and placers of the Nizhnii Tagil, Veresovyi Bor, and Kamenushenskii massifs (Table 5). They are observed as grains measuring ~20 µm and/or form chains subparallel to the boundaries of platinum-group mineral grains or their cracks (Fig. 14*d*). In Pt–Fe minerals from the Veresovyi Bor massif, we revealed single grains of osarsite replacing osmium (Table 5; Fig. 14*e*) and of ruarsite (Fig. 14*f*) in isoferroplatinum cracks.

The secondary minerals of the Veresovyi Bor massif include abundant Pb- and Te-containing minerals (Table 6). Lead-containing minerals are represented by single grains of xingzhongite present as metacrystals in isoferroplatinum (Fig. 15*a*). Plumbopalladinite and rhodplumsite (Fig. 15*b*, *c*, respectively) were found as finest individual grains in the complex aggregate of Pt–Fe minerals replacing isoferroplatinum, tetraferroplatinum, and tulameenite. Zvyagintsevite fills fine cracks in isoferroplatinum. The unnamed mineral compositionally similar to (Rh, Pt)Pb(Bi, Te)$_2$ was found as small (<20 µm) grains in isoferroplatinum cracks (Fig. 15*d*). Potarite was detected as small (<10 µm) grains intergrown with tetraferroplatinum (Fig. 15*e*). Extremely rare unnamed Pd–Cd–Hg minerals are present as inclusions <10 µm in size in an aggregate composed of Os–Ir intermetallic com-

Table 5. Composition of hexaferrum and PGE sulfides and sulfoarsenides developed after primary Pt–Fe minerals of the Veresovyi Bor (1–3, 5) and Nizhnii Tagil (4) massifs (wt.%)

No.	Fe	Ni	Cu	Rh	Pd	Os	Ir	Pt	As	S	Σ	Formula
1	16.1	–	–	1.55	–	79.4	–	–	0.91	–	97.9	$Os_{0.57}Fe_{0.39}Rh_{0.02}As_{0.02}$
2	12.1	–	–	1.30	–	79.8	3.97	–	1.34	–	98.5	$Os_{0.61}Fe_{0.31}Ir_{0.03}Rh_{0.02}As_{0.03}$
3	16.8	8.75	5.08	14.1	–	–	23.1	–	–	29.7	97.5	$(Fe_{2.93}Ni_{1.45}Rh_{1.33}Ir_{1.17}Cu_{0.78})_{7.65}S_{9.00}$
4	0.24	0.15	0.26	27.9	–	–	23.7	1.60	29.9	13.70	97.5	$(Rh_{0.66}Ir_{0.30}Pt_{0.02})_{0.98}As_{0.97}S_{1.03}$
5	–	–	–	4.64	–	47.2	9.33	7.42	11.5	21.3	101.4	Osarsite(?)

Note. 1, 2, hexaferrum, the formulae were calculated per 100 at.%; 3, ferhodsite, the formula was calculated per nine S atoms; 4, hollingworthite, the formula was calculated per three atoms.

Table 6. Chemical composition of Pb- and Te-containing secondary minerals of the Veresovyi Bor massif (wt.%)

No.	Fe	Cu	Pb	Bi	Rh	Pd	Ir	Pt	Hg	Te	S	Σ	Formula
1	1.79	4.70	17.1	–	11.7	–	37.1	4.00	–	–	20.0	96.4	$(Pb_{0.51}Cu_{0.45}Fe_{0.20})_{1.14}$ $(Ir_{1.19}Rh_{0.70}Pt_{0.13})_{2.02}S_{3.83}$
2	0.79	5.11	18.2	–	10.9	–	30.7	9.88	–	–	20.8	97.8	$(Pb_{0.53}Cu_{0.48}Ni_{0.14}Fe_{0.08})_{1.23}$ $(Ir_{0.96}Rh_{0.63}Pt_{0.30})_{1.89}S_{3.88}$
3	–	–	9.21	10.2	23.0	–	2.60	1.61	–	48.9	–	95.6	–
4	–	–	9.76	11.6	23.6	–	1.83	1.34	–	48.0	–	96.1	–
5	–	6.12	20.9	–	18.2	–	24.6	6.20	–	–	22.0	100.8	$(Pb_{0.56}Cu_{0.53}Ni_{0.26})_{1.35}$ $(Rh_{0.98}Ir_{0.71}Pt_{0.18})_{1.87}S_{3.79}$
6	3.66	–	–	–	–	31.1	–	9.79	53.10	–	–	97.7	$(Pd_{0.87}Pt_{0.15})_{1.01}Hg_{0.91}$

Note. Content of Ni: an. 2—1.35 wt.%, an. 5—2.74 wt.%. 1, 2, 5, xingzhongite, the formulas were calculated per seven atoms; 3, 4, unnamed mineral; 6, potarite, the formula was calculated per two atoms.

pounds and oxygen-containing Pt–Fe minerals replacing tetraferroplatinum (Fig. 15f). These minerals have the following composition (wt.%): Fe = 2.13 and 1.63, Cu = 0.67 and 0.63, Pd = 39.38 and 37.85, Cd = 19.07 and 18.96, Hg = 35.68 and 34.87, at points 7 and 8, respectively (Fig. 15f, at point 7, Ag reaches 3.65), with calculated formulas: $(Pd_{1.89}Fe_{0.20}Cu_{0.05}Pt_{0.08})_{2.22}Cd_{0.87}Hg_{0.91}$ и $(Pd_{1.82}Ag_{0.17}Fe_{0.15}Pt_{0.07}Cu_{0.05})_{2.22}Cd_{0.86}Hg_{0.89}$.

DISCUSSION

The sequence of mineral formation in chromitites of zoned clinopyroxenite–dunite massifs is considered in many publications (Zavaritskii, 1928; Betekhtin, 1935; Rudashevskii, 1987; Genkin, 1997; Pushkarev et al., 2007; Volchenko et al., 2007; Tolstykh et al., 2011, 2015; Mochalov, 2013; Stepanov, 2015). In most cases, the sequence of mineral formation was studied for samples from the Nizhnii Tagil massif (Zavaritskii, 1928; Malitch et al., 2014). The significant difference between platinum-group mineral assemblages in chromitites of different Middle Urals massifs does not provide a general idea of the sequence of mineral formation. However, a considerable amount of data has been accumulated during the long-term investigation into platinum-group mineralization. Based on these data, invoking additional information about the morphology of aggregates and individual grains, and using statistically significant samples of analyses of minerals from different clinopyroxenite–dunite massifs, it is possible to substantiate the model of the evolution of platinum-group mineralization most correctly. For example, a volumetric morphologic analysis in the course of our research made it possible to recognize induction surfaces on platinum and Cr-spinel grains, which unambiguously indicate the co-growth of the minerals. This phenomenon cannot be detected in flat sections because of the great diversity of forms of platinum-group minerals and their different relations with Cr-spinel.

The performed study of the relations among platinum-group minerals in chromitites has shown that Os–Ir–Ru alloys, laurite, erlichmanite, kashinite, bowieite, and thiospinels are the earliest minerals. They occur mostly as euhedral grains in Pt–Fe minerals. These minerals, along with isoferroplatinum, tetraferroplatinum, and ferronickelplatinum, were assigned by Pushkarev et al. (2007) to an early paragenesis. Tolstykh et al. (2011) attribute isoferroplatinum, Os–Ir–Ru alloys, laurite, and erlichmanite to a magmatic paragenesis, which is confirmed by our research. We include kashinite, bowieite, and Ir–Rh thiospinels into the same paragenesis. The study of the sequence of mineral formation has shown that osmium crystallized before Cr-spinel, as evidenced by its euhedral crystals trapped by Cr-spinel. These crystals formed over the entire period of Cr-spinel crystallization preceding the formation of Pt–Fe minerals.
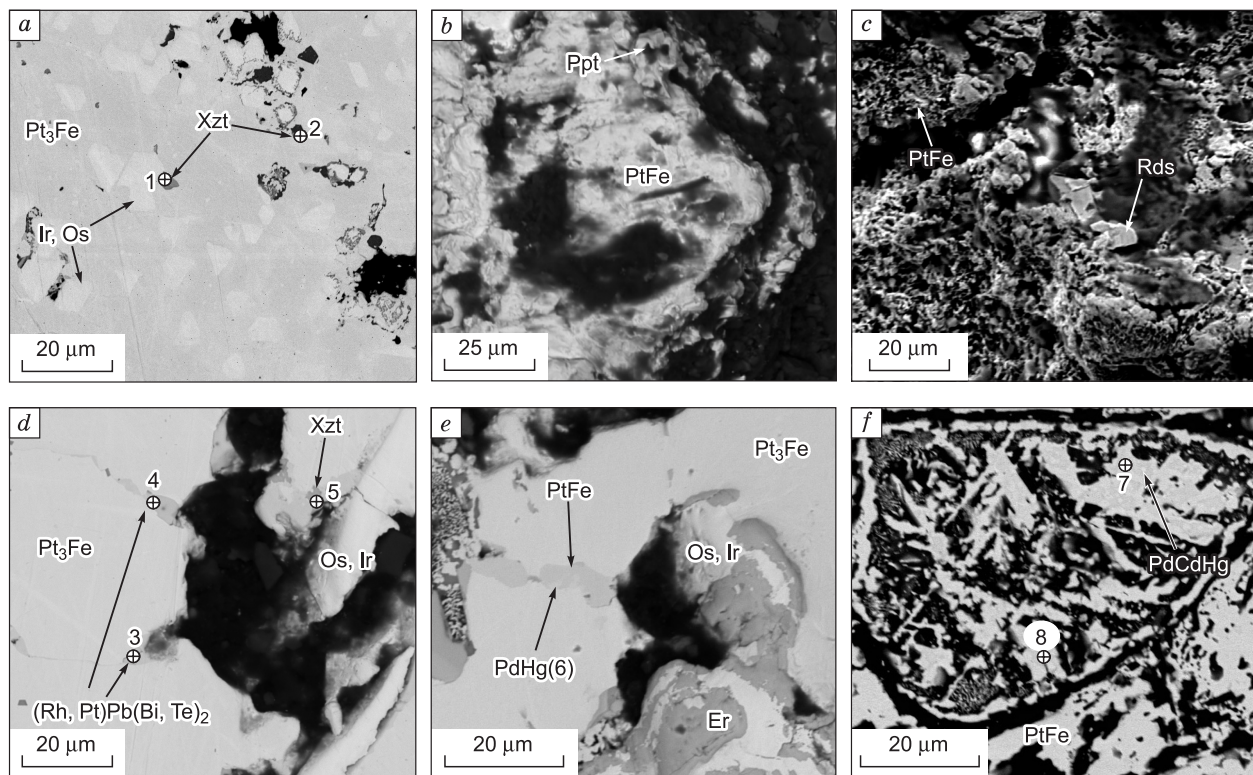
Fig. 15. Latest secondary minerals of the Veresovyi Bor massif. Xzt, xingzhongite, Ppt, plumbopalladinite, Rds, rhodplumsite, (Rh, Pt)Pb(Bi, Te)$_2$, unnamed mineral, PdHg, potarite, PdCdHg, unnamed mineral. Numbers of analytical points follow Table 6. SEM (BSE mode) images.

At the final stages of Cr-spinel crystallization, iridium, laurite–erlichmanite, and kashinite–bowieite crystallized. The possibility of melt crystallization of osmium, iridium, and laurite was confirmed by experiments (Brenan and Andrews, 2001). The attribution of minerals of the series kashinite–bowieite to a magmatic paragenesis is debatable, but the individual grains of these minerals have the same relations with isoferroplatinum and Cr-spinel as laurite. Brenan and Andrews (2001) report that Ir sulfide behaves similarly to erlichmanite during crystallization, and Peregoedova and Ohnenstetter (2002) assign kashinite, bowieite, erlichmanite, and laurite to the same paragenesis. The magmatic nature of Ir–Rh thiospinels also raises many questions, but our research has shown that their morphologic features (first of all, the presence of these minerals as euhedral crystals in isoferroplatinum) and the existence of CuRh$_2$S$_4$ and Rh$_2$S$_3$ in equilibrium assemblage at 900 ºC (Makovicky et al., 1993) permit attributing them to the same paragenesis with laurite, erlichmanite, kashinite, and bowieite. In most cases, these minerals are euhedral with respect to isoferroplatinum, but the boundaries of the outer growth zones of their grains in flat sections sometimes resemble co-growth surfaces. Single mineral grains contain pseudomorphs of kashinite (Fig. 11d) and erlichmanite (Fig. 15e) developed after osmium plates, which indicates an increase in sulfur fugacity during the melt crystallization. The PGE sulfide grains show a distinct compositional evolution: Laurite at the grain edges

is replaced by erlichmanite, and bowieite, by kashinite, which is due to an increase in sulfur activity (Zaccarini et al., 2018).

The morphologic features of Pt–Fe alloys corresponding in composition to isoferroplatinum and ferroplatinum give grounds to state that they formed together with Cr-spinel. This is evidenced by the numerous induction surfaces typical of co-growing minerals (Popov, 2011). Taking into account the earlier proposed model (Betekhtin, 1935; Tolstykh et al., 2011), it is reasonable to assign these Pt–Fe minerals to paragenesis originated at the magmatic stage of formation of clinopyroxenite–dunite massifs at temperatures of 1310–1090 ºC (Zaccarini et al., 2018). The combination of the morphologic features of minerals of magmatic paragenesis (Kozlov et al., 2019), first of all, the wide development of the induction surfaces of platinum-group minerals and rock-forming minerals (by analogy with platinum-group minerals from South Urals placers (Zaikov et al., 2017)), indicates a significant contribution of eutectic liquids (melts) to the crystallization of minerals.

Our study of the series of Pt–Fe alloys has shown that ferroplatinum is the first to crystallize and then isoferroplatinum forms. These data correspond to the sequence of mineral formation proposed for dunites of the Svetlyi Bor massif and chromitites of the Kamenushenskii massif (Tolstykh et al., 2011). The sequence of crystallization of Pt–Fe minerals is due to an increase in oxygen fugacity during the mag-

matic process (Amosse et al., 2000). The regularities established on comparison of Pt–Fe minerals from dunites and later chromitites are undoubtedly related to an increase in f_{O_2}, which agrees with the conclusions drawn by Zaccarini et al. (2018). The significant difference in the distribution of ferroplatinum and isoferroplatinum in chromitites from different massifs suggests different conditions of formation of the dunite "core" containing chromitite veins and, probably, different depths of dunite crystallization.

Pt–Fe alloys crystallize from melt with different amounts of Ir. Initially, Ir is dissolved in Pt–Fe alloys; a temperature decrease to 845 ºC (Savitskii, 1984) leads to a breakdown of the alloys. Analysis of the contents of the breakdown products has revealed the following regularity: These products are abundant in isoferroplatinum and scarce in ferroplatinum. Thus, we have confirmed the earlier established division of minerals formed at the magmatic stage into the Pt–Fe–Os paragenesis with a predominance of ferroplatinum and the isoferroplatinium–iridium paragenesis (Tolstykh et al., 2002, 2005).

The magmatic stage of the formation of platinum-group mineralization in chromitites was terminated with the crystallization of ferroplatinum and isoferroplatinum. Subsequent mineral formation consisted in the replacement of primary minerals by newly formed ones. The end of melt crystallization is evidenced by brittle deformations of pinacoid osmium crystals and plastic deformations of Pt–Fe minerals caused by active tectonic transformations of dunites and Pt-containing chromitites in the solid state. The absence of signs of deformation in secondary minerals of the tetraferroplatinum group indicates their formation after the active tectonic transformation of dunites and chromitites containing platinum-group minerals.

Judging from the type of replacement of primary Pt–Fe minerals, the studied ferronickelplatinum, tulameenite, and tetraferroplatinum belong to a later paragenesis formed at the postmagmatic stage of the formation of chromite–platinum mineralization, which agrees with the data of most researchers (Genkin, 1997; Tolstykh et al., 2011; Malitch et al., 2014). We have established that tulameenite is developed after ferroplatinum, and ferronickelplatinum aggregates, after a mineral compositionally corresponding to isoferroplatinum. Tetraferroplatinum replacing tulameenite in chromitites from the Veresovyi Bor massif is the latest mineral. Part of mineral inclusions from magmatic paragenesis was replaced at the late stage. For example, kashinite–bowieite was replaced by a fine-crystalline aggregate of different Pt–Fe minerals. Tulameenite and Fe and Ni sulfides are also present in this aggregate. Finally, the minerals of the isomorphic series kashinite–bowieite were replaced by an unnamed mineral with the formula Pt_3IrRh (Tolstykh et al., 2011). Osmium was replaced by hexaferrum. Laurite was replaced by complex ruthenium oxide with Os impurity. The Pt–Fe minerals were partly replaced by oxides (Pushkarev et al., 2007; Tolstykh et al., 2011; Zaccarini et al., 2018). The formation of the above paragenesis is undoubtedly related to

active serpentinization of dunites, which agrees with other concepts of platinum-group mineralization in chromitites of clinopyroxenite–dunite complexes of the Middle Urals (Betekhtin et al., 1935; Genkin, 1997).

At the final stages of the evolution of chromite–platinum ore systems, a paragenesis with a predominance of PGE sulfides (cooperite and ferhodsite), sulfoarsenides (irarsite, hollingworthite, osarsite, and ruarsite), plumbides (zvyagintsevite and rhodplumsite), and amalgams (potarite) and Pb- and Te-containing minerals formed. Their individual grains and aggregates of these minerals metasomatically replaced both minerals of the magmatic paragenesis and minerals resulted from serpentinization.

Thus, the ontogenesis of platinum-group mineralization in chromitites of zoned clinopyroxenite–dunite massifs of the Middle Urals is divided into two stages: magmatic and postmagmatic. The postmagmatic stage is divided into two substages (Fig. 16).

The formation of dunites of the Urals Platinum Belt is a debatable issue. However, the recent data on the U–Pb zircon age of dunites (Malitch et al., 2009) and the modal $^{187}Os/^{188}Os$ ages of laurite and Os–Ir–(Ru) alloys (Malitch et al., 2014) support the viewpoint of Efimov (2009), who proposed a mechanism of tectonic intrusion of late Riphean dunite bodies into the structure of dunite–clinopyroxenite–gabbro complexes. Hence, the study of Ordovician magmatites hosting dunites does not permit modeling of the processes of dunite crystallization, which significantly complicates the understanding of their genesis. Some researchers (Johan 2002; Tolstykh et al., 2011, 2015; Simonov et al., 2013, 2017) believe that dunites formed during the differentiation of picritic melts with liquation separation of an oxide–ore phase of predominantly chromite composition (Okrugin, 2004). With regard to the genetic relations between the minerals in dunites and Pt-containing chromitites, this model seems to be the most reasonable.

According to the results of dating, the dunites formed during the late Riphean rifting within the incipient Urals folded area, similarly to clinopyroxenite–dunite massifs of the Aldan Shield, which are spatially associated with continental rifts (Efimov and Tavrin, 1978). Picritic magmatism is more typical of rift structures (Abramovich, 1997) rather than suprasubduction volcanic arcs, whose evolution in the Ordovician was accompanied by the formation of structural rock complexes of the Urals Platinum Belt.

One of the important details clarifying the ontogenesis of platinum-group mineralization in chromitites of clinopyroxenite–dunite massifs of the Middle Urals is the propagation of brittle deformations in Cr-spinels and osmium and of plastic deformations in Pt–Fe minerals. Probably, these deformations reflect the general serious tectonic transformations of dunites at the stage of the tectonic transformation of dunite–clinopyroxenite–gabbro complexes during the formation of the Tagil–Magnitogorsk megazone. Zavaritskii (1928), however, associated the brittle and plastic deformations in Cr-spinels and platinum-group minerals with ser-
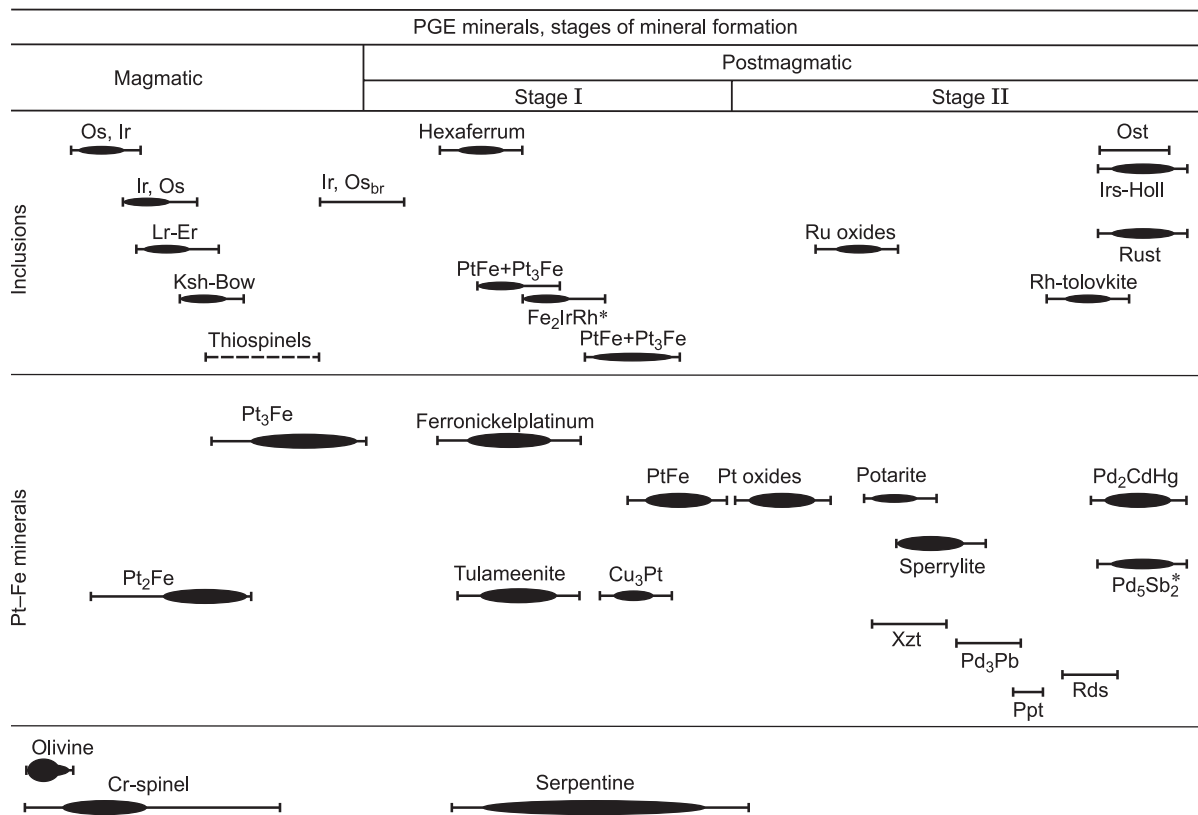
Fig. 16. Scheme of the sequence of formation of platinum-group minerals in chromitites of clinopyroxenite–dunite massifs of the Middle Urals, after Stepanov (2015). Asterisks mark minerals given after Tolstykh et al. (2011). Lr, laurite; Er, erlichmanite; Ksh, kashinite; Bow, bowieite; Ost, osarsite; Irs, irarsite; Holl, hollingworthite; Rust, ruarsite; Xzt, xingzhongite; Ppt, plumbopalladinite; Rds, rhodplumsite; Pd_3Pb, zvyagentsevite. Ir, Os_{exs}, breakdown of solid solution of iridium in isoferroplatinum; dashed line shows the assumed time interval of mineral formation.

pentinization of dunites. Taking into account that clinopyroxenite–dunite massifs were localized in the subduction zone in the Early Paleozoic, where they were subjected to hydrothermal activity and underwent intense serpentinization (Ivanov, 2011), we assume that the tectonic transformations were combined with metasomatic transformations. It is the bulk strong metasomatic transformation of dunites and their serpentinization that led to the formation of secondary minerals replacing primary magmatic Pt–Fe minerals and of inclusions in them.

The formation of minerals at the second postmagmatic stage (PGE sulfoarsenides, plumbides, amalgams, and sulfides and Hg-containing minerals, due to the supply of As, Sb, and Hg atypical of ultrabasic rocks) was probably contributed by fluids generated during the late tectonomagmatic activity. For example, dunites of the Kamenushenskii massif are intruded by granites of Silurian age (Ivanov, 1997) containing vein bodies of garnet–tourmaline–muscovite granite pegmatites. Similar, much younger (relative to the rocks of the ultramafic–mafic association) intrusions are spread in the proximity of most of clinopyroxenite–dunite massifs of the Middle Urals. It was these intrusions that might have initiated the last stage of serpentinization with the supply of As, Sb, Hg, and other elements. The elucidation of this issue requires a special study.

CONCLUSIONS

Taking into account all the obtained data, we have recognized two stages of the formation of platinum-group mineralization: magmatic and postmagmatic. The postmagmatic stage is divided into two substages, based on the significantly different chemical compositions of the formed minerals. We have established platinum-group mineral assemblages formed at each stage and substage: (1) magmatic minerals, comprising Os–Ir–Ru intermetallic compounds, sulfides of the series erlichmanite–laurite and kashinite–bowieite, Ir–Rh thiospinels, and Fe–Pt minerals, with a predominance of isoferroplatinum and ferroplatinum; (2) late platinum-group minerals, with a predominance of tetraferroplatinum, tulameenite, and ferronickelplatinum; and (3) secondary minerals, formed at the final stage of serpentinization, with a predominance of PGE sulfides, sulfoarsenides, plumbides, and amalgams.

Based on the ontogenetic examination of platinum-group minerals and the analysis of the general tectonic position and geologic structure of the massifs, with regard to the earlier published data (Efimov, 2009), including the results of dating of platinum-group minerals (Malitch et al., 2009, 2014), we assume that the minerals of the magmatic para-

genesis (first of all, most of the Pt–Fe minerals) formed as a result of intrusions during rifting.

The performed study has proved that the formation of secondary minerals replacing platinum-group minerals of the magmatic paragenesis was initiated by serpentinization of dunites. The origin of the solutions that caused serpentinization is still debatable. The research has led us to the conclusion that the platinum-group mineral assemblage with a predominance of tetraferroplatinum–tulameenite–ferronickelplatinum is related to the formation of the Ural folded area, which proceeded along with the formation of island-arc systems in the Ordovician. This conclusion agrees with the geodynamic model of the formation of the Urals Platinum Belt proposed by Ivanov (2011). Minerals of the postmagmatic paragenesis formed at the Paleozoic island-arc stage of formation of zoned clinopyroxenite–dunite massifs, which was recognized by a comprehensive study of platinum-bearing rocks of the Nizhnii Tagil massif (Tessalina et al., 2015). At present, it is impossible to say unambiguously what caused the formation of late minerals of the postmagmatic paragenesis. However, we assume that dunites of the zoned massifs were repeatedly subjected to serpentinization, which is consistent with the intricate tectonic history of the Urals Platinum Belt. To establish the relationship between different assemblages of platinum-group minerals and different stages of serpentinization requires a special detailed study.

REFERENCES

Abramovich, I.I., 1997. The Fundamentals of Geodynamic Analysis during Geological Mapping [in Russian]. Izd. VSEGEI, St. Petersburg.

Amosse, J., Dable, P., Allibert, M., 2000. Thermochemical behaviour of Pt, Ir, Rh, and Ru vs f_{O2} and f_{S2} in a basaltic melt. Implications for the differentiation and precipitation of these elements. Mineral. Petrol. 68, 29–62.

Anikina, E.V., Malitch, K.N., Pushkarev, E.V., Shmelev, V.R., 2014. The Nizhny Tagil and Volkovsky Massifs of the Uralian Platinum Belt, and Related Deposits. Field Trip Guidebook. 12th International Platinum Symposium. IGG UB RAS, Yekaterinburg.

Auge, T., Genna, A., Legendre, O., Ivanov, K.S., Volchenko, Yu.A., 2005. Primary platinum mineralization in the Nizhny Tagil and Kachkanar ultramafic complexes, Urals, Russia: A genetic model for PGE concentration in chromite-rich zones. Econ. Geol. 100, 707–732.

Begizov, V.D., Zav'yalov, E.N., 2016. Ferhodsite (Fe, Rh, Ir, Ni, Cu, Co, Pt)$_{9-x}$S$_8$, a new mineral from the Nizhnii Tagil ultrabasic massif. Novye Dannye o Mineralakh 51, 8–11.

Begizov, V.D., Zav'yalov, E.N., Khvostova, V.P., 1976. Minerals of the series erlichmanite–laurite and hollingworthite–irarsite from Urals placers. Zapiski VMO 105 (2), 213–218.

Betekhtin, A.G., 1935. Platinum and Other Platinum-Group Minerals [in Russian]. Izd. AN SSSR, Moscow.

Brenan, J., Andrews, D., 2001. High-temperature stability of laurite and Ru–Os–Ir alloy and their role in PGE fractionation in mafic magmas. Can. Mineral. 39 (2), 341–360.

Britvin, S.N., Dolivo-Dobrovol'skii, D.V., Krzhizhanovskaya, M.G., 2017. Software for processing X-ray powder pattern data obtained with a Rigaku RAXIS Rapid II diffractometer with a cylindrical detector. Zapiski RMO 146 (3), 104–107.

Cabri, L.J., Feather, C.E., 1975. Platinum–iron alloys: nomenclature based on a study of natural and synthetic alloys. Can. Mineral. 13 (2), 117–126.

Duparc, L., Tikhonowitch, M., 1920. Le Platine et les Gites Platiniferes de l'Oural et du Monde. Geneve.

Efimov, A.A., 2009. Urals Platinum Belt: current ideas of the geology, nature, and history of formation of the unique Russian object, in: Ultrabasic–Basic Complexes of Folded Areas and Associated Deposits [in Russian]. IGG UrO RAN, Yekaterinburg, Vol. 1, pp. 176–179.

Efimov, A.A., Tavrin, I.F., 1978. The genetic unity of platinum-bearing dunites of the Urals and the Aldan Shield. Dokl. Akad. Nauk SSSR 243 (4), 991–994.

Genkin, A.D., 1997. Sequence and conditions of formation of platinum-group minerals in the Nizhnii Tagil dunite massif. Geologiya Rudnykh Mestorozhdenii 39 (1), 41–48.

Harris, D.C., Cabri, L.J., 1991. Nomenclature of platinum-group-element alloys: Review and revision. Can. Mineral. 29 (2), 231–237.

Ivanov, K.S., 2011. Genesis of chromium–platinum ore mineralization of the Uralian (Nizhnii Tagil) type. Dokl. Earth Sci. 441 (1), 1489–1491.

Ivanov, O.K., 1997. Concentric Zoned Pyroxenite–Dunite Massifs of the Urals [in Russian]. Izd. Ural'skogo Universiteta, Yekaterinburg.

Johan, Z., 2002. Alaskan-type complexes and their platinum-group element mineralization, in: Cabri, L.J. (Ed.), The Geology, Geochemistry and Mineral Beneficiation of Platinum-Group Elements. Canadian Institute of Mining, Metallurgy and Petroleum, Montreal, Vol. 54, pp. 669–719.

Johan, Z., Ohnenstetter, M., Fisher, W., Amosse, J., 1990. Platinum-group minerals from the Durance River Alluvium, France. Mineral. Petrol. 42, 287–306.

Karpinsky, A.P., 1893. Primary platinum deposit in the Urals. Zapiski Akademii Nauk 71, 222–229.

Karpinsky, A.P., 1926. The probable origin of primary platinum deposits of the Urals type. Izvestiya Akad. Nauk SSSR. Ser. 6 20 (1–2), 159–170.

Kashin, S.A., Kozak, S.S., Nikolaeva, L.A., Tikhomirov, K.P., 1956. Mineralogy and Petrochemistry of Platinum-Bearing Rocks of the Middle Urals and Some Regularities of Platinum Distribution [in Russian]. NII NIGRIZoloto MTsM SSSR, Moscow.

Kozlov, A.P., Chanturiya, V.A., Sidorov, E.G., Tolstykh, N.D., Telegin, Yu.M., 2011. Large-volume platinum ore deposits in zonal mafic–ultramafic complexes of the Ural–Alaskan type and the outlook for their development. Geol. Ore Deposits 53 (5), 374–389.

Kozlov, A.V., Stepanov, S.Yu., Palamarchuk, R.S., Minibaev, A.M., 2019. Ontogenetic basis for choosing a model for the formation of PGE mineralization in zoned clinopyroxenite-dunite massifs in the Urals. Zapiski RMO 148 (2), 115–130.

Kutyrev, A.V., Sidorov, E.G., Antonov, A.V., Chubarov, V.M., 2018. Platinum-group mineral assemblage of the Prizhimny Creek (Koryak Highland). Russian Geology and Geophysics (Geologiya i Geofizika) 59 (8), 935–944 (1164–1175).

Lazarenkov, V.G., Malitch, K.N., Sakh'yanov, L.O., 1992. Platinum-Group Mineralization of Zoned Ultrabasic and Komatiite Massifs [in Russian]. Nedra, Leningrad.

Legendre, O., Auge, T., 1992. Alluvial platinum-group minerals from the Manampotsy area, East Madagascar. Austral. J. Earth Sci. 39, 389–404.

Lokerman, A.A., 1982. The Story of the Most Resistant Elements [in Russian]. Znanie, Moscow.

Makovicky, M., Makovicky, E., Rose-Hansen, J., 1993. The phase system Rh–Ni–Fe–S (Fe:Ni = 1:1) at 900 ºC and 500 ºC, in: IAGOD Symposium, France, Orleans: Terra Abstr., Vol. 3.

Malakhov, I.A., Malakhova, L.V., 1970. The Nizhnii Tagil Pyroxenite–Dunite Massif and the Enclosing Rocks [in Russian]. Izd. UFAN SSSR, Sverdlovsk.

Malitch, K.N., Thalhammer, O.A.R., 2002. Pt–Fe nuggets derived from clinopyroxenite–dunite massifs, Russia: a structural, compositional and osmium-isotope study. Can. Mineral. 40 (2), 395–418.

Malitch, K.N., Efimov, A.A., Ronkin, Yu.L., 2009. Archean U–Pb isotope age of zircon from dunite of the Nizhny Tagil massif (the Uralian Platinum Belt). Dokl. Earth Sci. 427 (1), 851–855.

Malitch, K.N., Badanina, I.Yu., Belousova, E.A., Khiller, V.V., 2014. Chemical composition and osmium isotope systematization of noble-metal mineralization of the zoned Nizhnii Tagil massif (Sverdlovsk Region, Russia). Trudy IGG UrO RAN, Issue 161, 316–321.

Malitch, K.N., Stepanov, S.Yu., Badanina, I.Yu., Khiller, V.V., 2015. Assemblages of platinum-group minerals of the Svetlyi Bor, Veresovyi Bor, and Nizhnii Tagil clinopyroxenite–dunite massifs of the Middle Urals. Vestnik UrO RMO, No. 12, 65–83.

Mochalov, A.G., 2013. A genetic model of PGM hosted in cumulative gabbro–pyroxenite–dunite complexes of the Koryak Highland, Russia. Geol. Ore Deposits 55 (3), 145–161.

Mosin, K.I., 2002. History of Platinum Mining in the Urals [in Russian]. Nizhneturinskaya Tipografiya, Nizhnyaya Tura.

Nixon, G., Cabri, L.J., Laflamme, J.H.G., 1990. Platinum-group-element mineralization in lode and placer deposits associated with the Tulameen Alaskan-type complex, British Columbia. Can. Mineral. 28, 503–535.

Okrugin, A.V., 2004. Crystallization–liquation model of formation of PGE-chromite ores in mafic–ultramafic complexes. Tikhookeanskaya Geologiya 23 (2), 63–75.

Palamarchuk, R.S., Stepanov, S.Yu., 2016. Native iridium of the Svetlyi Bor clinopyroxenite–dunite massif (Middle Urals), in: Proceedings of the Conference "Ural Mineralogical School 2016" [in Russian]. IMin UrO RAN, Miass, pp. 81–84.

Peregoedova, A., Ohnenstetter, M., 2002. Collectors of Pt, Pd and Rh in a S-poor Fe–Ni–Cu sulfide system at 760 ºC: experimental data and application to ore deposits. Can. Mineral. 40 (2), 527–561.

Podlipskii, M.Yu., Sidorov, E.G., Tolstykh, N.D., Krivenko, A.P., 1999. Cobalt-bearing malanite and other Pt-thiospinels from the Maior River placers (Kamchatka). Geologiya i Geofizika (Russian Geology and Geophysics 40 (4), 645–648 (629–632).

Popov, V.A., 2011. Practical Genetic Mineralogy [in Russian]. Izd. UrO RAN, Yekaterinburg.

Pushkarev, E.V., Anikina, E.V., Garuti, G., Zaccarini, F., 2007. Cr–Pt mineralization of the Nizhnii Tagil type in the Urals: structural and chemical characteristics and problem of genesis. Litosfera, No. 3, 28–65.

Ramdohr, P., 1969. The Ore Minerals and Their Intergrowths. Pergamon Press, Oxford.

Rudashevskii, N.S., 1987. Origin of platinum-group mineralization of different types in rocks of ultramafic associations. Zapiski VMO 116 (2), 222–235.

Savitskii, E.M. (Ed.), 1984. Noble Metals [in Russian]. Metallurgiya, Moscow.

Sidorov, E.G., Kozlov, A.P., Tolstykh, N.D., 2012. The Gal'moenan Basic–Ultrabasic Massif and Its Platinum Content [in Russian]. Nauchnyi Mir, Moscow.

Sidorov, E.G., Kutyrev, A.V., Zhitova, S., Chubarov, M., Khanin, D., 2019. Origin of platinum-group mineral assemblages from placer in rivers draining from the Ural-Alaskan type Itchayvayamsky Ultramafics, Far East Russia. Can. Mineral. 57 (1), 91–114.

Simonov, V.A., Puchkov, V.N., Prikhod'ko, V.S., Stupakov, S.I., Kotlyarov, A.V., 2013. Conditions of crystallization of dunite from the Nizhnii Tagil platinum-bearing ultrabasic massif (Urals). Dokl. Earth Sci. 449 (2), 451–454.

Simonov, V.A., Vasil'ev, Yu.R., Kotlyarov, A.V., Prikhod'ko, V.S., 2017. Evolution of magmatic melts during the formation of platinum-bearing ultrabasic massifs on the Siberian Platform, in: Geology and Minerageny of Northern Eurasia. Proceedings of the Meeting Dedicated to the 60th Anniversary of the Institute of Geology and Geophysics [in Russian]. IPTs NGU, Novosibirsk, pp. 215–216.

Stepanov, S.Yu., 2015. Ontogenesis of platinum-group minerals of zoned ultramafic massifs (Middle Urals), in: Proceedings of the Conference "Ontogenesis, Phylogenesis, and System of Mineralogy" [in Russian]. IMin UrO RAN, Miass, pp. 182–186.

Stepanov, S.Yu., Malich, K.N., 2016. Genesis of tulameenite and ferronickelplatinum from chromitites of clinopyroxenite–dunite massifs of the Central Urals, in: Metallogeny of Ancient and Modern Oceans—2016. From Mineral Genesis to Deposits [in Russian]. IMin UrO RAN, Miass, pp. 228–232.

Stepanov, S.Yu., Pilyugin, A.G., Zolotarev, A.A., 2015. Comparative characteristics of the compositions of platinum-group minerals in chromitites and placers of the Nizhnii Tagil massif, Middle Urals. Zapiski Gornogo Instituta 211 (1), 22–28.

Stepanov, S.Yu., Palamarchuk, R.S., Varlamov, D.A., Kozlov, A.V., Khanin, D.A., Antonov, A.V., 2018. Platinum-group minerals from the deluvial placer in the Veresovka River, Veresovyi Bor clinopyroxenite-dunite massif (Middle Urals). Zapiski RMO 147 (5), 40–60.

Stepanov, S.Yu., Palamarchuk, R.S., Kozlov, A.V., Khanin, D.A., Varlamov, D.A., Kiseleva, D.V., 2019. Platinum-group minerals of Pt-placer deposits associated with the Svetloborsky Ural-Alaskan type massif, Middle Urals, Russia. Minerals 9 (2), 77.

Stepanov, S.Yu., Malich, K.N., Kozlov, A.V., Badanina, I.Yu., Antonov, A.V., 2017. Platinum group element mineralization of the Svetly Bor and Veresovy Bor clinopyroxenite–dunite massifs, Middle Urals, Russia. Geol. Ore Deposits 59 (3), 244–255.

Telegin, Yu.M., Telegina, T.V., Tolstykh, N.D., 2009. Geologic specifics of platinum ore occurrences in the Svetlyi Bor and Kamenushenskii massifs of the Urals Platinum Belt, in: Ultrabasic–Basic Complexes of Folded Areas and Associated Deposits. Proceedings of the Third International Conference [in Russian]. IGG UrO RAN, Yekaterinburg, Vol. 2, pp. 212–215.

Tessalina, S.G., Malitch, K.N., Auge, T., Puchkov, V.N., Belousova, E., McInnes, B.I.A., 2015. Origin of the Nizhny Tagil clinopyroxenite–dunite massif, Uralian Platinum Belt, Russia: Insights from PGE and Os isotope systematics. J. Petrol. 56 (12), 2295–2318.

Tolstykh, N., Krivenko, A., Sidorov, E., Laajoki, K., Podlipsky, M., 2002. Ore minerology of PGM placers in Siberia and the Russian Rar East. Ore Geol. Rev. 20 (1), 1–25.

Tolstykh, N., Sidorov, E.G., Krivenko, A.P., 2005. Platinum-group element placers associated with Ural–Alaska type complexes, in: Mineral. Ass. Can. Short Course 35, Oulu, Finland, pp. 113–143.

Tolstykh, N.D., Telegin, Yu.M., Kozlov, A.P., 2011. Platinum mineralization of the Svetloborsky and Kamenushinsky massifs (Urals Platinum Belt). Russian Geology and Geophysics (Geologiya i Geofizika) 52 (6), 603–619 (775–793).

Tolstykh, N., Kozlov, A., Telegin, Yu., 2015. Platinum mineralization of the Svetly Bor and Nizhny Tagil intrusions, Urals Platinum Belt. Ore Geol. Rev. 67, 234–243.

Trushin, S.I., Osetskii, A.I., Cherepanov, A.V., Korneev, A.V., 2017. Search for ore platinum in the Urals by drilling large-diameter boreholes, in: Razvedka i Okhrana Nedr, No. 2, 40–42.

Volchenko, Yu.A., Ivanov, K.S., Koroteev, V.A., Auge, T., 2007. Structural and petrologic evolution of complexes of the Urals Platinum Belt during the formation of Urals-type chromite–platinum deposits. Litosfera, No. 4, 73–101.

Vysotskii, N.K., 1913. Platinum deposits in the Is and Nizhnii Tagil regions, Urals. Transactions of the Geological Committee. New Series [in Russian]. St. Petersburg, No. 62.

Weiser, T., Schmidt-Thome, M., 1993. Platinum-group minerals from the Santiago River, Esmeraldas province, Ecuador. Can. Mineral. 31, 61–73.

Zaccarini, F., Garuti, G., Pushkarev, E., Thalhammer, O., 2018. Origin of platinum group minerals (PGM) inclusions in chromite deposits of the Urals. Minerals 8, 1–21.

Zaikov, V.V., Popov, V.A., Zaikova, E.V., Blinov, I.A., Kotlyarov, V.A., 2017. Composition and morphology of crystals of platinum-group minerals from South Urals placers. Mineralogiya 3 (4), 51–56.

Zaitsev, A.M., 1898. Platinum Deposits in the Urals [in Russian]. Izd. Dom M.N. Kononova i I.F. Skulimovskogo, Tomsk.

Zavaritskii, A.N., 1928. Primary Platinum Deposits in the Urals [in Russian]. Izd. Geologicheskogo Komiteta, Leningrad.

Zoloev, K.K., Volchenko, Yu.A., Koroteev, V.A., Malakhov, I.A., Mardiros'yan, A.N., Khrypov, V.N., 2001. Platinum-Group Mineralization in Geologic Complexes of the Urals [in Russian]. OAO Ural'skaya Geologo-S''emochnaya Ekspeditsiya, Yekaterinburg.

Editorial responsibility: V.N. Sharapov